The chiral Gaussian two-matrix ensemble of real asymmetric matrices

2010 J. Phys. A: Math. Theor. 43 085211

(http://iopscience.iop.org/1751-8121/43/8/085211)

IOP PUBLISHING JOURNAL OF PHYSICS A: MATHEMATICAL AND THEORETICAL

J. Phys. A: Math. Theor. **43** (2010) 085211 (29pp) doi:10.1088/1751-8113/43/8/085211

The chiral Gaussian two-matrix ensemble of real asymmetric matrices

G Akemann[1], M J Phillips[1] and H-J Sommers[2]

[1] Department of Mathematical Sciences and BURSt Research Centre, Brunel University West London, Uxbridge UB8 3PH, UK
[2] Fakultät für Physik, Universität Duisburg-Essen, 47048 Duisburg, Germany

E-mail: Gernot.Akemann@brunel.ac.uk

Received 13 November 2009, in final form 8 January 2010
Published 8 February 2010
Online at stacks.iop.org/JPhysA/43/085211

Abstract

We solve a family of Gaussian two-matrix models with rectangular $N \times (N+\nu)$ matrices, having real asymmetric matrix elements and depending on a non-Hermiticity parameter μ. Our model can be thought of as the chiral extension of the real Ginibre ensemble, relevant for Dirac operators in the same symmetry class. It has the property that its eigenvalues are either real, purely imaginary or come in complex conjugate eigenvalue pairs. The eigenvalue joint probability distribution for our model is explicitly computed, leading to a non-Gaussian distribution including K-Bessel functions. All n-point density correlation functions are expressed for finite N in terms of a Pfaffian form. This contains a kernel involving Laguerre polynomials in the complex plane as a building block which was previously computed by the authors. This kernel can be expressed in terms of the kernel for *complex* non-Hermitian matrices, generalizing the known relation among ensembles of Hermitian random matrices. Compact expressions are given for the density at finite N as an example, as well as its microscopic large-N limits at the origin for fixed ν at strong and weak non-Hermiticity.

PACS numbers: 02.10.Yn, 11.15.Ha, 05.45.−a

(Some figures in this article are in colour only in the electronic version)

1. Introduction

Non-Hermitian random matrix theory (RMT) introduced by Ginibre [1] is almost as old as its Hermitian counterpart. At first it was seen as an academic exercise to drop the Hermiticity constraint and thus to allow for complex eigenvalues. However, in the past two decades, we have seen many applications of such RMTs featuring complex eigenvalues precisely for physical reasons, and we refer to [2] for examples and references. Because matrices with real data are often modelled by RMT, one could view the real Ginibre ensemble of asymmetric

matrices as being the most interesting non-Hermitian ensemble. Unfortunately, it has also turned out to be the most difficult one, as it took over 25 years to compute the joint distribution of its eigenvalues [3, 4], being real or coming in complex conjugate pairs. The integrable structure and all eigenvalue correlation functions were computed only very recently for the real Ginibre ensemble [5–11].

Our motivation for generalizing this model is as follows. In the 1990s, Verbaarschot proposed extending the three classical (and Hermitian) ensembles of Wigner and Dyson to the so-called chiral RMT [12], in order to describe the low energy sector of quantum chromodynamics (QCD) and related field theories. These chiral ensembles are also known as Wishart or Laguerre ensembles. Their non-Hermitian extensions [13, 14] were motivated by adding a chemical potential for the quarks, which breaks the anti-Hermiticity of the Dirac operator in field theory. It was observed numerically quite early [14] that these chiral versions of the Ginibre ensembles have distinct features, either attracting eigenvalues to the real and imaginary axes (real matrices), repelling them (quaternion real matrices) or having no such symmetry (complex matrices). Only later was it realized how to solve these chiral non-Hermitian RMTs analytically, by using replicas [15] or by extending the initial one-matrix model plus a constant symmetry-breaking term [13, 14] to a two-matrix model. This idea from Osborn [16] led to a complex eigenvalue model that can be solved using orthogonal polynomials in the complex plane [17]. The solution of the two-matrix model was then derived for complex [16, 18] and quaternion real matrices [19]. Our paper aims to solve the third and most difficult of such non-Hermitian RMTs, a chiral two-matrix model of real asymmetric matrices introduced in our previous work [20]. For more details on RMT applications to the QCD-like Dirac operator spectrum, we refer to [21].

Many more non-Hermitian RMTs than just the three Ginibre ensembles and their chiral (or Wishart/Laguerre) counterparts exist [22] and these are mostly unsolved to date. Very recently another two-matrix model generalization of the real Ginibre ensemble was introduced and solved in [23]. There the eigenvalue correlations of the *ratio* of two quadratic matrices are sought, whereas here we deal with the *product* of two rectangular matrices. Whilst the former case leads to a Cauchy-type weight function, in our model we will obtain a weight of Bessel-K functions for the eigenvalues. We hope that given the plethora of RMT applications, our particular model will find applications beyond the field theory that it has been designed for.

The approach of solving our model is based on the variational method detailed in [7, 10]. It follows its two main ideas: first to compute the joint probability distribution function (jpdf) for general N by reducing it to 2×2 and 1×1 blocks. Because we are considering rectangular matrices, this is *a priori* not guaranteed to work. Second, we use the variational method [7, 10] in combining all density correlations with n points (being real, purely imaginary or complex conjugates) into a single Pfaffian form. This reduces the computation to determining its main building block, an anti-symmetric kernel. Whilst it can be deduced from the spectral 1-point density—which was known for the real Ginibre ensemble [24]—we here exploit an idea from our previous publication [20]. There the kernel was determined by computing the expectation value of two characteristic polynomials using Grassmannians. The same relation between kernel and characteristic polynomials is known to hold for the symmetry classes with complex [25] or quaternion real matrices [19], in fact for any class of non-Gaussian weight functions.

As a new result, we can express our kernel for real asymmetric matrices in terms of the kernel for complex non-Hermitian matrices. Such a relation might have been expected to exist as it is known for Hermitian RMT [26, 27].

Other methods that have been successfully applied to the real Ginibre ensemble, such as the supersymmetric method [28], skew-orthogonal polynomials [8] or probabilistic methods [9], are very likely to be extendible to our two-matrix model as well.

The paper is organized as follows. In section 2, we summarize our main statements: the definition of the matrix model, its jpdf in terms of the real, imaginary and complex conjugate eigenvalue pairs, and the solution for all density correlation functions as a Pfaffian of a matrix-valued kernel. Examples are given for the simplest spectral densities at finite N and in the microscopic large-N limits for strong and for weak non-Hermiticity at the origin. These findings are then detailed in section 3 on the jpdf, where we separately treat $N = 1, 2$ and general N. The spectral density correlations and their finite- and large-N results are derived and illustrated in section 4. Our conclusions are presented in section 5. Some technical details on the computation of the Jacobian are collected in appendix A.

2. Summary of results

2.1. The model

The chiral Gaussian ensemble of real asymmetric matrices as introduced by the authors [20] is given by a two-matrix model of rectangular matrices P and Q of sizes $N \times (N+\nu)$ with real elements, without further symmetry restriction. The partition function normalized to unity is given by

$$\mathcal{Z} = \left(\frac{1}{\sqrt{2\pi}}\right)^{2N(N+\nu)} \int_{\mathbb{R}^{N(N+\nu)}} \mathrm{d}P \int_{\mathbb{R}^{N(N+\nu)}} \mathrm{d}Q \exp\left[-\frac{1}{2}\,\mathrm{Tr}\,(PP^T + QQ^T)\right], \tag{2.1}$$

where we integrate over all the independent, normally distributed matrix elements of P and Q. We are interested in the eigenvalues of the matrix $\mathcal{D}$ of size $2N + \nu$ squared

$$\mathcal{D} \equiv \begin{pmatrix} \mathbf{0}_{N\times N} & P + \mu Q \\ P^T - \mu Q^T & \mathbf{0}_{(N+\nu)\times(N+\nu)} \end{pmatrix} \equiv \begin{pmatrix} \mathbf{0}_{N\times N} & A \\ B^T & \mathbf{0}_{(N+\nu)\times(N+\nu)} \end{pmatrix}. \tag{2.2}$$

Here $\mu \in (0, 1]$ is the non-Hermiticity parameter, interpolating between the chGOE ($\lim \mu \to 0$) and maximal non-Hermiticity ($\mu = 1$). The analogous chiral Gaussian two-matrix models with unitary and symplectic symmetry were introduced in [16, 19], respectively.

In applications to field theory, $\mathcal{D}$ corresponds to the chiral Dirac operator, and μ to the chemical potential[3]. Typically, N_f extra determinants of the type $\det[\mathcal{D} + m I_{2N+\nu}]$ are inserted into the partition function (2.1), where m is the quark mass, but we will restrict ourselves in this paper to the case $N_f = 0$; this is referred to as the quenched case.

For later convenience, we give an equivalent form of equation (2.1), by changing variables from

$$P = \tfrac{1}{2}(A + B), \qquad Q = \tfrac{1}{2\mu}(A - B), \tag{2.3}$$

to matrices A and B defined in equation (2.2):

$$\mathcal{Z} = \left(\frac{1}{4\pi\mu}\right)^{N(N+\nu)} \int_{\mathbb{R}^{N(N+\nu)}} \mathrm{d}A \int_{\mathbb{R}^{N(N+\nu)}} \mathrm{d}B\, \mathrm{e}^{-\frac{1}{2}\eta_+ \mathrm{Tr}\,(AA^T+BB^T)+\frac{1}{2}\eta_- \mathrm{Tr}\,(AB^T+BA^T)} \tag{2.4}$$

$$\text{with} \quad \eta_\pm \equiv \frac{1 \pm \mu^2}{4\mu^2}. \tag{2.5}$$

The two μ-dependent combinations $\eta_\pm$ will be used throughout the paper.

[3] The Euclidian Dirac operator in field theory is actually anti-Hermitian for $\mu = 0$, but we will not use this convention here.

2.2. *Eigenvalue representation*

The eigenvalues Λ of the Dirac matrix $\mathcal{D}$ are determined from the following equation[4]:

$$0 = \det[\Lambda I_{2N+\nu} - \mathcal{D}] = \Lambda^{\nu} \det[\Lambda^2 I_N - AB^T] = \Lambda^{\nu} \prod_{j=1}^{N} \left(\Lambda^2 - \Lambda_j^2\right). \tag{2.6}$$

For this reason we will first compute the eigenvalue distribution of the $N \times N$ Wishart-type combination of matrices $C \equiv AB^T$. C has real elements, and therefore its eigenvalues Λ_j^2 are real, or else come in complex conjugate pairs. The matrix $\mathcal{D}$ itself has the following solutions: ν zero-eigenvalues $\Lambda = 0$, and $2N$ eigenvalues coming in pairs $\Lambda = \pm\Lambda_j$. Consequently the non-zero eigenvalues of $\mathcal{D}$ fall into three categories:

(i) for $\Lambda_j^2 > 0$: real pairs $\Lambda = \pm\Lambda_j \in \mathbb{R}$
(ii) for $\Lambda_j^2 < 0$: purely imaginary pairs $\Lambda = \pm\Lambda_j \in \mathrm{i}\mathbb{R}$
(iii) for pairs $\Lambda_j^2, \Lambda_j^{*2}$: quadruplets $\Lambda = \pm\Lambda_j, \pm\Lambda_j^* \in \mathbb{C}\backslash\{\mathbb{R} \cup \mathrm{i}\mathbb{R}\}$.

This leads to an accumulation of eigenvalues on both the real and the imaginary axes as already pointed out in [20]. The same phenomenon has been observed numerically in a one-matrix model [14] based on the proposal [13] (obtained from equation (2.1) by choosing $Q \sim I$). This is in contrast to the real Ginibre model where eigenvalues accumulate only on the real axis (see e.g. [29]).

The joint probability distribution (jpdf) for the matrix C is obtained from equation (2.4) by inserting a matrix delta function; using the cyclic property of the trace we then have

$$P(C) \sim \exp[\eta_- \operatorname{Tr} C] \int_{\mathbb{R}^{N(N+\nu)}} \mathrm{d}A \int_{\mathbb{R}^{N(N+\nu)}} \mathrm{d}B \exp\left[-\frac{\eta_+}{2} \operatorname{Tr}(AA^T + BB^T)\right] \delta(C - AB^T). \tag{2.7}$$

As shown in section 3, our final result for the jpdf of $\mathcal{D}$ in terms of squared variables $z_k = x_k + \mathrm{i}y_k \equiv \Lambda_k^2$ with $\mathrm{d}^2 z_k = \mathrm{d}x_k\, \mathrm{d}y_k$ is

$$\mathcal{Z} = \int_{\mathbb{C}} \mathrm{d}^2 z_1 \ldots \int_{\mathbb{C}} \mathrm{d}^2 z_N\, P_N(z_1, \ldots, z_N) \tag{2.8}$$

$$= c_N \prod_{k=1}^{N} \int_{\mathbb{C}} \mathrm{d}^2 z_k\, w(z_k) \prod_{i<j}^{N} (z_i - z_j) \sum_{n=0}^{[N/2]} \left(\prod_{l=1}^{n} (-2\mathrm{i}) \delta(x_{2l-1} - x_{2l}) \delta(y_{2l-1} + y_{2l}) \Theta(y_{2l-1}) \right.$$
$$\left. \times\, \Theta(x_1 > x_3 > \cdots > x_{2n-1}) \Theta(x_{2n+1} > x_{2n+2} > \cdots > x_N) \delta(y_{2n+1}) \ldots \delta(y_N) \right). \tag{2.9}$$

The integration measure $\mathrm{d}^2 z_k$ extends over the complex plane for *each* of the z_k. The normalization constant c_N will be given in equation (3.46). In equation (2.9) we sum over all distinct possibilities for N eigenvalues to come in $n \geqslant 0$ complex conjugate pairs, with the remaining $N - 2n \geqslant 0$ eigenvalues being real. For $n = 0$ in equation (2.9), the product in the first line is simply unity.

Specifically, the jpdf is only non-zero when the eigenvalues appear in the following order: the n complex eigenvalue pairs must be placed first, ordered with respect to decreasing

[4] This follows from equation (2.2) using the standard relation $\det \begin{pmatrix} a & b \\ c & d \end{pmatrix} = \det(d) \det(a - bd^{-1}c)$ for square matrices a and d, with d invertible.

real parts:[5]

$$\left(\mathrm{Im}\,\Lambda_1^2 > 0\right),\ \left(\mathrm{Re}\,\Lambda_2^2 = \mathrm{Re}\,\Lambda_1^2, \mathrm{Im}\,\Lambda_2^2 = -\mathrm{Im}\,\Lambda_1^2\right),\ \left(\mathrm{Re}\,\Lambda_3^2 \leqslant \mathrm{Re}\,\Lambda_2^2, \mathrm{Im}\,\Lambda_3^2 > 0\right), \ldots,$$
$$\left(\mathrm{Re}\,\Lambda_{2n-1}^2 \leqslant \mathrm{Re}\,\Lambda_{2n-2}^2, \mathrm{Im}\,\Lambda_{2n-1}^2 > 0\right),\ \left(\mathrm{Re}\,\Lambda_{2n}^2 = \mathrm{Re}\,\Lambda_{2n-1}^2, \mathrm{Im}\,\Lambda_{2n}^2 = -\mathrm{Im}\,\Lambda_{2n-1}^2\right), \tag{2.10}$$

and the $N - 2n \geqslant 0$ real eigenvalues follow, and are also ordered with respect to decreasing real parts:

$$\Lambda_{2n+1}^2 > \Lambda_{2n+2}^2 > \cdots > \Lambda_N^2. \tag{2.11}$$

The function $g(z)$ inside the weight function

$$w(z) \equiv |z|^{\nu/2} \exp[\eta_- z] g(z) \tag{2.12}$$

depends on whether z ($\equiv \Lambda^2$) is real or complex:

$$g(z) \equiv 2K_{\frac{\nu}{2}}(\eta_+|z|) \qquad \text{for} \quad z \in \mathbb{R}, \tag{2.13}$$

$$[g(z)]^2 = \left[g(z^*)\right]^2 \equiv 2\int_0^\infty \frac{\mathrm{d}t}{t}\, \mathrm{e}^{-2\eta_+^2 t(x^2-y^2)-\frac{1}{4t}} K_{\frac{\nu}{2}}\left(2\eta_+^2 t(x^2+y^2)\right) \mathrm{erfc}(2\eta_+\sqrt{t}|y|)$$
$$\text{for} \quad z = x + \mathrm{i}y \in \mathbb{C}. \tag{2.14}$$

Because the complex eigenvalues come in pairs, we will always get *two* factors $g(z)$ for each pair (note the square on the left-hand side of definition (2.14)). The limit $y \to 0$ of a single $g(z)$ in equation (2.14) is smooth, leading to equation (2.13).

The essential idea in the derivation of the jpdf detailed in section 3 is to reduce the calculation of the jpdf for $\mathcal{D}$ with general N down to 2×2 and 1×1 blocks, which can be handled in terms of the $N = 2$ and $N = 1$ problems which we solve explicitly.

2.3. Density correlation functions for finite N

We follow the method of using a generating functional for all eigenvalue density correlation functions introduced in [7, 10]. Because we essentially follow [7, 10], we can be brief here. We enlarge the definition of the partition function (2.9) by introducing sources $f\left(\Lambda_k^2\right)$[6]:

$$\mathcal{Z}[f] \equiv \int_{\mathbb{C}} \mathrm{d}^2 z_1 \ldots \int_{\mathbb{C}} \mathrm{d}^2 z_N\, P_N(z_1, \ldots, z_N) f(z_1) \ldots f(z_N). \tag{2.15}$$

For pairwise distinct arguments $z_1 \neq z_2 \neq \cdots \neq z_n$, the n-point density correlation functions are then generated in terms of functional derivatives with respect to the sources, leading to insertions of delta functions $\frac{\delta f(z)}{\delta f(z')} = \delta^2(z - z')$:

$$R_n(z_1, \ldots, z_n) = \frac{\delta}{\delta f(z_1)} \cdots \frac{\delta}{\delta f(z_n)} \mathcal{Z}[f]\Big|_{f\equiv 1}. \tag{2.16}$$

In doing so, each n-point function contains a sum of different contributions, splitting n into all possible combinations of real eigenvalues and complex eigenvalue pairs. Both the generating functional $\mathcal{Z}[f]$ and the n-point density R_n, can be written as Pfaffians [6, 7]:

$$\mathcal{Z}[f] = c_N\, \mathrm{Pf}\left[\int_{\mathbb{C}} \mathrm{d}^2 z_1 \int_{\mathbb{C}} \mathrm{d}^2 z_2 f(z_1) f(z_2) \mathcal{F}(z_1, z_2) z_1^{i-1} z_2^{j-1}\right]_{1\leqslant i,j\leqslant N}, \tag{2.17}$$

[5] Unlike for real eigenvalues, two complex eigenvalues that are not complex conjugates can have the same real part, without the jpdf vanishing. Although being of measure zero, we can fix this ambiguity by ordering with respect to decreasing the absolute imaginary part.

[6] These will symmetrize the ordered eigenvalues when differentiating.

$$R_n(z_1,\ldots,z_n) \equiv \frac{N!}{(N-n)!}\int_{\mathbb{C}} \mathrm{d}^2 z_{n+1}\ldots\int_{\mathbb{C}} \mathrm{d}^2 z_N\, P_N(z_1,\ldots,z_N)$$
$$= \mathrm{Pf}\begin{bmatrix} \mathcal{K}_N(z_i,z_j) & -G_N(z_i,z_j) \\ G_N(z_j,z_i) & -W_N(z_i,z_j)\end{bmatrix}_{1\leqslant i,j\leqslant n}. \tag{2.18}$$

In the latter case, one has to compute the Pfaffian of the ordinary, $2n\times 2n$ matrix composed of the matrix of quaternions inside the square bracket. We have restricted ourselves to even N for simplicity. The case of odd N can be treated along the lines of [10] (or [11] for an alternative formulation). We have introduced the following functions of two complex variables $z_j = x_j + \mathrm{i}y_j$, $j = 1, 2$:

$$\mathcal{F}(z_1,z_2) = w(z_1)w(z_2)(2\mathrm{i}\delta^2(z_1-z_2^*)\mathrm{sgn}(y_1) + \delta(y_1)\delta(y_2)\mathrm{sgn}(x_2-x_1)), \tag{2.19}$$

$$\mathcal{K}_N(z_1,z_2) = \frac{\eta_-}{8\pi(4\mu^2\eta_+)^{\nu+1}}$$
$$\times\sum_{j=0}^{N-2}\left(\frac{\eta_-}{\eta_+}\right)^{2j}\frac{(j+1)!}{(j+\nu)!}\left\{L_{j+1}^{\nu}\left(\frac{z_2}{4\mu^2\eta_-}\right)L_j^{\nu}\left(\frac{z_1}{4\mu^2\eta_-}\right) - (z_1\leftrightarrow z_2)\right\} \tag{2.20}$$
$$= \frac{\eta_-}{8\pi(4\mu^2\eta_+)^{\nu+1}}\left(z_2\frac{\partial}{\partial z_2} - z_1\frac{\partial}{\partial z_1} - \frac{z_2-z_1}{4\mu^2\eta_-}\right)$$
$$\times\sum_{j=0}^{N-2}\left(\frac{\eta_-}{\eta_+}\right)^{2j}\frac{j!}{(j+\nu)!}L_j^{\nu}\left(\frac{z_1}{4\mu^2\eta_-}\right)L_j^{\nu}\left(\frac{z_2}{4\mu^2\eta_-}\right), \tag{2.21}$$

$$G_N(z_1,z_2) = -\int_{\mathbb{C}}\mathrm{d}^2 z\,\mathcal{K}_N(z_1,z)\mathcal{F}(z,z_2), \tag{2.22}$$

$$W_N(z_1,z_2) = -\mathcal{F}(z_1,z_2) + \int_{\mathbb{C}}\mathrm{d}^2 z\int_{\mathbb{C}}\mathrm{d}^2 z'\mathcal{F}(z_1,z)\mathcal{K}_N(z,z')\mathcal{F}(z',z_2). \tag{2.23}$$

The kernel $\mathcal{K}_N(z_1,z_2)$ is the building block of all correlations and is actually defined in terms of $\mathcal{F}(z_1,z_2)$ (see section 4 for further details). However, we will give a different proof of the precise form of equation (2.20) which does not rely on direct evaluation of the definition; rather, it will be calculated from the expectation value of two characteristic polynomials (see also [20]). Note that in equation (2.21) we have expressed the kernel of our real two-matrix model ($\beta = 1$) as a derivative of the kernel of the complex two-matrix model [16] ($\beta = 2$). We found that a similar relation holds relating the kernel of the $\beta = 1$ real Ginibre ensemble [8, 20] to the one for the $\beta = 2$ complex Ginibre ensemble [30], containing Hermite polynomials in the complex plane.

There is an integration theorem in analogy to other matrix models with complex eigenvalues [7, 26, 31]:

$$\int_{\mathbb{C}}\mathrm{d}^2 z_n \mathrm{Pf}\begin{bmatrix} \mathcal{K}_N(z_i,z_j) & -G_N(z_i,z_j) \\ G_N(z_j,z_i) & -W_N(z_i,z_j)\end{bmatrix}_{1\leqslant i,j\leqslant n}$$
$$= (N-n+1)\mathrm{Pf}\begin{bmatrix} \mathcal{K}_N(z_i,z_j) & -G_N(z_i,z_j) \\ G_N(z_j,z_i) & -W_N(z_i,z_j)\end{bmatrix}_{1\leqslant i,j\leqslant n-1}. \tag{2.24}$$

This is the major advantage of working with an n-point correlation function as defined in equation (2.18) which contains all possible contributions of real eigenvalues and complex conjugate eigenvalue pairs. Had we studied instead a particular n-point function with a fixed and given number of real and complex conjugate eigenvalues, we would have found that such a simple integration theorem does not exist [5].

Let us explain one example explicitly, the spectral density, which we will give for even N only. Details can be found in section 4 including figures, where we follow the method of [7, 10]. From equation (2.18), we have

$$R_1(z_1) = \int_{\mathbb{C}} \mathrm{d}^2 z \mathcal{K}_N(z_1, z)\mathcal{F}(z, z_1) \equiv R_1^{\mathbb{C}}(z_1) + \delta(y_1) R_1^{\mathbb{R}}(x_1). \tag{2.25}$$

Inserting the appropriate weight from equations (2.13) and (2.14) we obtain with $z = x + \mathrm{i}y$

$$R_1^{\mathbb{C}}(z) = -2\mathrm{i}|z|^{\nu}\, \mathrm{e}^{2\eta_- x}\mathrm{sgn}(y)\mathcal{K}_N(z, z^*) \tag{2.26}$$

$$\times\, 2\int_0^{\infty} \frac{\mathrm{d}t}{t} \exp\left[-2\eta_+^2 t(x^2 - y^2) - \frac{1}{4t}\right] K_{\frac{\nu}{2}}(2\eta_+^2 t(x^2 + y^2))\mathrm{erfc}(2\eta_+\sqrt{t}|y|),$$

$$R_1^{\mathbb{R}}(x) = \int_{-\infty}^{\infty} \mathrm{d}x' \mathrm{sgn}(x - x')|xx'|^{\frac{\nu}{2}}\, \mathrm{e}^{\eta_-(x+x')} 2K_{\frac{\nu}{2}}(\eta_+|x|)2K_{\frac{\nu}{2}}(\eta_+|x'|)\mathcal{K}_N(x, x'). \tag{2.27}$$

Equations (2.25)–(2.27) are valid for even N only. In the final step we can change from squared variables $z = x + \mathrm{i}y = \Lambda^2$ to Dirac eigenvalues Λ, using the simple transformations

$$\begin{aligned} R_{1\mathrm{Dirac}}^{\mathbb{C}}(z) &= 4|z|^2 R_1^{\mathbb{C}}(z^2), \\ R_{1\mathrm{Dirac}}^{\mathbb{R}}(x) &= 2|x| R_1^{\mathbb{R}}(x^2). \end{aligned} \tag{2.28}$$

Note that the latter describes the density both of real Dirac eigenvalues, for $R_{1\,\mathrm{Dirac}}^{\mathbb{R}}(x)$ with $x \in \mathbb{R}$, and of purely imaginary Dirac eigenvalues, for $R_{1\,\mathrm{Dirac}}^{\mathbb{R}}(x)$ with $x \in \mathrm{i}\,\mathbb{R}$. Because $R_1^{\mathbb{R}}(x^2) \neq R_1^{\mathbb{R}}(-x^2)$, this is not the same function; see e.g. figure 2 in section 4.

2.4. The large-N limit

In order to take the large-N limit in principle, one first has to rescale all eigenvalues in equation (2.9) $\Lambda_k \to \sqrt{N}\,\Lambda_k$, which is equivalent to giving all the matrix elements in equation (2.1) Gaussian weights $\exp[-(N/2)\,\mathrm{Tr}\,P^T P]$ for P, and similarly for Q. In this parametrization, the macroscopic spectral density will have a compact support in the large-N limit, given by a circle for $\mu = 1$, and an ellipse for $0 < \mu < 1$. We will not discuss this macroscopic limit in detail but will focus on the local correlations, i.e. the microscopic large-N limit. Here one has to distinguish between strong and weak non-Hermiticity [32], each of which involves a second rescaling.

We first give the strong non-Hermiticity limit *after* the first rescaling, defined by keeping μ fixed and only rescaling the eigenvalues according to

$$\lim_{N\to\infty, \Lambda\to 0} N\Lambda^2 \equiv \lambda^2. \tag{2.29}$$

This scaling actually cancels the first scaling. Because of this, the scaling limit is also true away from the origin.

We only give the microscopic kernel here, to be inserted into equations (2.26) and (2.27). For $\mu = 1$, the kernel simplifies to monic powers; see equation (33) in [20]. Its large-N limit is easily seen to lead to a modified Bessel function

$$\mathcal{K}_{\nu}^{S}(z_1, z_2) = \frac{(z_1 - z_2)}{64\pi 2^{\nu}} \sum_{j=0}^{\infty} \frac{1}{j!(j+\nu)!} \left(\frac{z_1 z_2}{4}\right)^j = \frac{(z_1 - z_2)}{64\pi}(z_1 z_2)^{-\nu/2} I_{\nu}(\sqrt{z_1 z_2}). \tag{2.30}$$

Because μ is not scaled here, in contrast to the weak limit below, the insertion into equations (2.26) and (2.27) is relatively straightforward, apart from the phase for negative real eigenvalues. The case for general μ which can also be obtained by simply rescaling the arguments in equation (2.30) is discussed in section 4, where we also show plots.

The weak non-Hermiticity limit at the origin (again *after* the initial rescaling above) is defined by scaling both the squared Dirac eigenvalues Λ^2 and the chemical potential μ^2 with $2N$, corresponding to the volume in field theory:

$$\lim_{N\to\infty,\mu\to 0} 2N\mu^2 \equiv \alpha^2, \qquad \lim_{N\to\infty,\Lambda\to 0} (2N)^2\Lambda^2 \equiv \lambda^2. \tag{2.31}$$

In this limit, the macroscopic density is projected back onto the real axis, with probability density given by the semi-circle as for $\mu = 0$ (when our model is Hermitian), whilst microscopically the eigenvalues still extend into the complex plane.

The limiting microscopic kernel, as a function of squared variables $z = \Lambda^2$, can be expressed in terms of our completely unscaled finite-N kernel as

$$\begin{aligned}\mathcal{K}^W(z_1,z_2) &\equiv \lim_{N\to\infty}\left[\frac{1}{(4N)^2}\left(\frac{z_1z_2}{(4N)^2}\right)^{\nu/2}\mathcal{K}_N\left(\frac{z_1}{4N},\frac{z_2}{4N};\mu=\frac{\alpha}{\sqrt{2N}}\right)\right]\\ &= \frac{1}{256\pi\alpha^2}\int_0^1 \mathrm{d}s\, s^2\,\mathrm{e}^{-2\alpha^2s^2}\{\sqrt{z_1}J_{\nu+1}(s\sqrt{z_1})J_\nu(s\sqrt{z_2})-(z_1\leftrightarrow z_2)\}\end{aligned} \tag{2.32}$$

which is to be inserted into the definition of the density (2.25). From equation (2.26), we obtain for the microscopic density of complex eigenvalues

$$\begin{aligned}\rho_\nu^{\mathbb{C}W}(z) &= -2\mathrm{i}\,\mathrm{sgn}(y)\,\exp\left[\frac{x}{4\alpha^2}\right]\mathcal{K}^W(z,z^*)\\ &\quad\times 2\int_0^\infty\frac{\mathrm{d}t}{t}\exp\left[-\frac{t(x^2-y^2)}{32\alpha^4}-\frac{1}{4t}\right]K_{\frac{\nu}{2}}\left(\frac{t(x^2+y^2)}{32\alpha^4}\right)\mathrm{erfc}\left(\frac{\sqrt{t}|y|}{4\alpha^2}\right).\end{aligned} \tag{2.33}$$

The real eigenvalue density is more subtle; we again refer to section 4 for a more detailed discussion of the weak limit, including figures.

3. Calculation of the joint probability distribution function

In this section, we compute the joint probability density function (jpdf) as stated in equation (2.9) for the squared non-zero eigenvalues of $\mathcal{D}$. For pedagogical reasons, we first compute the jpdf separately for $N = 1$ and 2 in sections 3.1 and 3.2, respectively. This is because we will need these results when treating the general N case in section 3.3, as these sub-blocks will appear in the computation of the general Jacobian. Some technical details will be deferred to appendix A. The cases with $N = 1, 2$ will make the parametrization and residual symmetries more transparent for later.

3.1. The $N = 1$ case

In this simplest case, our matrices P and Q, or after changing variables A and B in equation (2.3), are of size $1 \times (1 + \nu)$ and are thus given by vectors $\mathbf{a}$ and $\mathbf{b}$, each of length $\nu + 1$. The eigenvalue equation (2.6) for $\mathcal{D}$ becomes

$$0 = \Lambda^\nu(\Lambda^2 - \mathbf{a}\cdot\mathbf{b}), \tag{3.1}$$

and thus we only have a single non-zero (and real) eigenvalue Λ^2 to determine. Its (j)pdf is given by

$$P(\Lambda^2) = \frac{1}{(4\pi\mu)^{\nu+1}}\int_{\mathbb{R}^{\nu+1}}\mathrm{d}\mathbf{a}\int_{\mathbb{R}^{\nu+1}}\mathrm{d}\mathbf{b}\exp[\eta_-\mathbf{a}\cdot\mathbf{b}]\exp\left[-\frac{\eta_+}{2}(|\mathbf{a}|^2+|\mathbf{b}|^2)\right]\delta(\Lambda^2-\mathbf{a}\cdot\mathbf{b}). \tag{3.2}$$

We simplify this expression in two steps. First, without loss of generality, we may choose the direction of $\mathbf{b}$ as the first basis vector for $\mathbf{a}$ in Cartesian coordinates. This leads to a decoupling

of the remaining components $a_2, \ldots, a_{\nu+1}$, and the integral now only depends on $\mathbf{b}$ through its modulus $b = |\mathbf{b}|$. Second, we choose polar coordinates for the vector $\mathbf{b}$, leading to the Jacobian b^ν, and, on symmetrically extending the integral over b to $-\infty$, we obtain

$$P(\Lambda^2) = \frac{1}{(4\pi\mu)^{\nu+1}} \frac{2\pi^{(\nu+1)/2}}{\Gamma\left(\frac{\nu+1}{2}\right)} \left(\frac{2\pi}{\eta_+}\right)^{\nu/2} \mathrm{e}^{\eta_-\Lambda^2} \frac{1}{2} \int_{-\infty}^{\infty} \mathrm{d}a_1 \int_{-\infty}^{\infty} \mathrm{d}b\, \mathrm{e}^{-\frac{1}{2}\eta_+(a_1^2+b^2)} \delta(\Lambda^2 - a_1 b)|b|^\nu$$
$$= \frac{1}{2^{3\nu/2+2}\mu^{\nu+1}\eta_+^{\nu/2}\sqrt{\pi}\Gamma\left(\frac{\nu+1}{2}\right)} \mathrm{e}^{\eta_-\Lambda^2} \int_{-\infty}^{\infty} \mathrm{d}b\, \mathrm{e}^{-\frac{1}{2}\eta_+(b^2+\Lambda^4/b^2)}|b|^{\nu-1}. \tag{3.3}$$

The first new pre-factor comes from the surface area of the unit ν-sphere

$$S_\nu \equiv \frac{2\pi^{(\nu+1)/2}}{\Gamma\left(\frac{\nu+1}{2}\right)} = \frac{\mathrm{VO}(\nu+1)}{\mathrm{VO}(\nu)} \tag{3.4}$$

(with $\mathrm{VO}(\nu)$ being the volume of the orthogonal group) through the angular integration over $\mathbf{b}$, the final pre-factor from the Gaussian integrations over the decoupled components of $\mathbf{a}$. It is important to note that the first line of equation (3.3) looks like a reduction to the $\nu = 0$ case, apart from the extra factor $|b|^\nu$ from the Jacobian. We will use the same strategy for $N = 2$ in the following subsection. In the next step, we change variables $\mathrm{e}^t = b^2/|\Lambda^2|$ to arrive at

$$P(\Lambda^2) = \frac{1}{2^{3\nu/2+2}\mu^{\nu+1}\eta_+^{\nu/2}\sqrt{\pi}\Gamma\left(\frac{\nu+1}{2}\right)} |\Lambda|^\nu \mathrm{e}^{\eta_-\Lambda^2} 2 \int_0^{\infty} \cosh(\nu t/2)\, \mathrm{e}^{-\eta_+|\Lambda^2|\cosh t}\, \mathrm{d}t$$
$$= \frac{1}{2^{3\nu/2+2}\mu^{\nu+1}\eta_+^{\nu/2}\sqrt{\pi}\Gamma\left(\frac{\nu+1}{2}\right)} |\Lambda|^\nu \mathrm{e}^{\eta_-\Lambda^2} 2K_{\frac{\nu}{2}}(\eta_+|\Lambda^2|). \tag{3.5}$$

Here we have used a particular representation equation, 9.6.24 in [33], of the K-Bessel function. It directly gives $c_{N=1}$ times the weight function in equations (2.12) and (2.13) when changing variables $\Lambda^2 \to z$, where

$$c_{N=1} = \frac{1}{2\pi} \frac{1}{(2\pi)^{\nu/2}(2\mu)^{\nu+1}\eta_+^{\nu/2}} \frac{S_\nu}{S_0}. \tag{3.6}$$

This is consistent with equations (2.9), (2.12) and (2.13), and ends our calculation for $N = 1$.

As a remark, equation (3.5) can be derived in various different ways, including Fourier transformation. It is known that if a and b are independent random variables with normal distributions, then the product $c = ab$ has the distribution function $P_0 \sim K_0$. Consequently, the sum of $\nu + 1$ (independent) such variables c_i has a distribution given by the convolution of $\nu + 1$ functions K_0. Fourier transformation F turns this into an ordinary product, and so we obtain $P_\nu = F^{-1}\{(F(P_0))^{\nu+1}\} \sim K_{\frac{\nu}{2}}$, i.e. on performing the integrals we again reach equation (3.5).

3.2. The $N = 2$ case

Our matrices A and B are now given by two row vectors $\mathbf{a}_{j=1,2}$ and $\mathbf{b}_{j=1,2}$ each of length $\nu+2$:

$$A = \begin{pmatrix} \mathbf{a}_1 \\ \mathbf{a}_2 \end{pmatrix}, \qquad B = \begin{pmatrix} \mathbf{b}_1 \\ \mathbf{b}_2 \end{pmatrix}, \qquad C = AB^T = \begin{pmatrix} \mathbf{a}_1 \cdot \mathbf{b}_1 & \mathbf{a}_1 \cdot \mathbf{b}_2 \\ \mathbf{a}_2 \cdot \mathbf{b}_1 & \mathbf{a}_2 \cdot \mathbf{b}_2 \end{pmatrix}. \tag{3.7}$$

The eigenvalue equation (2.6)

$$0 = \Lambda_\nu \det[\Lambda^2 I_2 - AB^T] \tag{3.8}$$

has two solutions $\Lambda_{1,2}^2$ which may (i) both be real or (ii) form a complex conjugate pair. We will have to distinguish these two cases below.

For the first step we reduce the calculation of $P(C)$ in equation (2.7) to a matrix integral of 2×2 matrices A' and B' times a Jacobian, as we did for $N = 1$ in the first line of equation (3.3). The resulting Jacobian here will be $\sim|\det B'|^{\nu}$. Our aim is to rotate both $\mathbf{b}_1$ and $\mathbf{b}_2$ into the xy-plane of the coordinates for the $\mathbf{a}_j$, as then

$$\mathbf{a}_i \cdot \mathbf{b}_j = \sum_{k=1}^{\nu+1} a_{ik} b_{jk} = a_{i1} b'_{j1} + a_{i2} b'_{j2}, \tag{3.9}$$

and the remaining components of the $\mathbf{a}_j$ decouple. Here we use primed vectors and coordinates to denote the quantities after rotation.

For $\nu = 1$ the corresponding Jacobian is obtained as follows. Rotating the 3D vector into 2D by $\mathbf{b}'_1 = O\,\mathbf{b}_1$ gives rise to a factor $\sim|\mathbf{b}_1|$. Alternatively it can be computed by comparing the initial and final 'volumes' (generalized surface areas, in fact), yielding $\frac{S_2|\mathbf{b}_1|^2}{S_1|\mathbf{b}_1|} = 2|\mathbf{b}_1|$, where S_n is given by equation (3.4). The remaining rotation around $\mathbf{b}_1$ rotates $\mathbf{b}_2$ into the xy-plane as well, giving $\frac{S_1|\mathbf{b}_2|\sin\theta}{S_0} = \pi|\mathbf{b}_2|\sin\theta$, in which $\theta \in [0, \pi]$ is the angle between $\mathbf{b}_1$ and $\mathbf{b}_2$. The final Jacobian reads

$$|\mathbf{b}_1||\mathbf{b}_2|\sin\theta = |\mathbf{b}'_1||\mathbf{b}'_2|\sin\theta = \begin{vmatrix} b'_{11} & b'_{12} \\ b'_{21} & b'_{22} \end{vmatrix} = |\det B'|, \tag{3.10}$$

where the last equality easily follows by parametrizing $\mathbf{b}'_1$ and $\mathbf{b}'_2$ in 2D, and the factor $\frac{S_2}{S_0}$ corresponds to the angular integration over $\mathbf{b}$.

For $\nu > 1$, we can thus successively repeat these steps by projecting onto one dimension lower until we reach the xy-plane. The volume factors will telescope out and we arrive at

$$\frac{S_\nu S_{\nu+1}}{S_0 S_1}(|\mathbf{b}'_1||\mathbf{b}'_2|\sin\theta)^{\nu} = \frac{S_\nu S_{\nu+1}}{S_0 S_1}|\det B'|^{\nu}. \tag{3.11}$$

We thus have reduced equation (2.7) for $N = 2$ from $2 \times (2+\nu)$ down to 2×2 matrices:

$$P(C) = \frac{c_{N=2}\eta_+}{2\pi^3}\,\mathrm{e}^{\eta_-\,\mathrm{Tr}\,C} \times \int_{\mathbb{R}^4} \mathrm{d}A' \int_{\mathbb{R}^4} \mathrm{d}B' \exp\left[-\frac{1}{2}\eta_+\,\mathrm{Tr}\,(A'A'^T + B'B'^T)\right] \delta(C - A'B'^T)|\det B'|^{\nu}, \tag{3.12}$$

where $c_{N=2}$ is defined in anticipation of the final result as

$$c_{N=2} = \frac{1}{8\pi}\,\frac{1}{(2\pi)^{\nu}(2\mu)^{4+2\nu}\eta_+^{\nu+1}}\,\frac{S_\nu S_{\nu+1}}{S_0 S_1}. \tag{3.13}$$

The Gaussian integrals over the decoupled components of the two vectors a_{jk} for $k > 2$ have been evaluated, using that $\mathrm{Tr}\,AA^T = |\mathbf{a}_1|^2 + |\mathbf{a}_2|^2$. The 2×2 matrix A' can now be integrated out, by formally changing variables $A' \to F = A'B'^T$ with the Jacobian $|\det B'|^{-2}$:

$$P(C) = \frac{c_{N=2}\eta_+}{2\pi^3}\,\mathrm{e}^{\eta_-\,\mathrm{Tr}\,C} \int_{\mathbb{R}^4} \mathrm{d}B' \exp\left[-\frac{1}{2}\eta_+\,\mathrm{Tr}\left(CC^T(B'B'^T)^{-1} + B'B'^T\right)\right] |\det B'|^{\nu-2}. \tag{3.14}$$

Note the similarity with equation (3.3).

In a second step, we perform the integral $\int \mathrm{d}B'$. Because CC^T is a symmetric, positive definite matrix, we can diagonalize it with an orthogonal transformation O

$$O^T(CC^T)O = \begin{pmatrix} \lambda_1 & 0 \\ 0 & \lambda_2 \end{pmatrix}, \qquad \lambda_{1,2} \geqslant 0. \tag{3.15}$$

Using the invariance of $\mathrm{d}B'$ we can change variables $B' \to OB'$ with $(B'B'^T)^{-1} \to O(B'B'^T)^{-1}O^T$. We thus replace CC^T by its diagonalized form equation (3.15) in the exponent in equation (3.14):

$$\mathrm{Tr}(B'B'^T + CC^T(B'B'^T)^{-1}) = a^2 + b^2 + c^2 + d^2 + h^{-2}((c^2+d^2)\lambda_1 + (a^2+b^2)\lambda_2), \tag{3.16}$$

where we have explicitly parametrized

$$B' \equiv \begin{pmatrix} a & b \\ c & d \end{pmatrix}, \qquad h \equiv \det B' = ad - bc. \tag{3.17}$$

We now introduce h as an independent variable in equation (3.14) by inserting a delta-function constraint in its integral representation:

$$\begin{aligned} P(C) &= \frac{c_{N=2}\eta_+}{4\pi^4}\,\mathrm{e}^{\eta_-\,\mathrm{Tr}C}\int_{-\infty}^{\infty}\mathrm{d}h|h|^{\nu-2}\int_{\mathbb{R}^4}\mathrm{d}B'\int_{-\infty}^{\infty}\mathrm{d}\omega\,\mathrm{e}^{-\mathrm{i}\omega(h-(ad-bc))} \\ &\quad\times\exp\left[-\frac{\eta_+}{2}[a^2+b^2+c^2+d^2+h^{-2}((c^2+d^2)\lambda_1+(a^2+b^2)\lambda_2)]\right] \\ &= \frac{c_{N=2}\eta_+}{4\pi^4}\,\mathrm{e}^{\eta_-\,\mathrm{Tr}\,C}2\int_0^{\infty}\mathrm{d}h\,h^{\nu-2}\int_{-\infty}^{\infty}\mathrm{d}\omega\,\mathrm{e}^{-\mathrm{i}\omega h}\frac{(2\pi)^2}{\omega^2+\eta_+^2(1+\lambda_1/h^2)(1+\lambda_2/h^2)}, \end{aligned} \tag{3.18}$$

where we performed the Gaussian integrals successively in pairs a, d and b, c, and switched to positive h. The denominator in the third line can be rewritten at the cost of an additional integral, $\frac{1}{a} = \int_0^{\infty}\mathrm{d}t\,\mathrm{e}^{-at}$ for $a > 0$, and after changing variables $\omega \to \tau = \omega h$, we have

$$\begin{aligned} P(C) &= \frac{2c_{N=2}\eta_+}{\pi^2}\,\mathrm{e}^{\eta_-\,\mathrm{Tr}\,C}\int_0^{\infty}\mathrm{d}h\,h^{\nu-1}\int_{-\infty}^{\infty}\mathrm{d}\tau\,\mathrm{e}^{-\mathrm{i}\tau}\int_0^{\infty}\mathrm{d}t\,\mathrm{e}^{-(\tau^2+\eta_+^2(h^2+(\lambda_1+\lambda_2)+\lambda_1\lambda_2/h^2))t} \\ &= \frac{2c_{N=2}\eta_+}{\pi^{3/2}}(\lambda_1\lambda_2)^{\nu/4}\,\mathrm{e}^{\eta_-\,\mathrm{Tr}\,C}\int_0^{\infty}\frac{\mathrm{d}t}{\sqrt{t}}\exp\left[-\eta_+^2(\lambda_1+\lambda_2)t-\frac{1}{4t}\right]K_{\frac{\nu}{2}}\left(2\eta_+^2\sqrt{\lambda_1\lambda_2}t\right). \end{aligned} \tag{3.19}$$

We performed the Gaussian integration over τ first, and then employed the following integral from equation 8.432.6 of [34]:

$$K_\nu(z) = \frac{1}{2}\left(\frac{z}{2}\right)^{\nu}\int_0^{\infty}\mathrm{d}t\,\frac{\mathrm{e}^{-t-z^2/4t}}{t^{\nu+1}} \tag{3.20}$$

to do the h-integration after another change of variables, arriving at our result (3.19).

As the final step we need to express $P(C)$ in terms of the eigenvalues of C (i.e. Λ_1^2 and Λ_2^2), rather than those of CC^T. This will also involve a Jacobian to be computed later. In equation (3.19), we need

$$\mathrm{Tr}\,C = \Lambda_1^2 + \Lambda_2^2, \qquad \lambda_1\lambda_2 = \det[CC^T] = \Lambda_1^4\Lambda_2^4, \tag{3.21}$$

which are trivial. Only the combination $\lambda_1 + \lambda_2 = \mathrm{Tr}(CC^T)$ requires more calculation. In general, we can orthogonally transform any real matrix C to the form

$$C = \begin{pmatrix} \sin\theta & -\cos\theta \\ \cos\theta & \sin\theta \end{pmatrix}\begin{pmatrix} \epsilon_1 & s \\ -s & \epsilon_2 \end{pmatrix}\begin{pmatrix} \sin\theta & \cos\theta \\ -\cos\theta & \sin\theta \end{pmatrix}, \tag{3.22}$$

where $\epsilon_1, \epsilon_2, s$ and the rotation parameter θ are all real. The matrix parameters $\{\epsilon_1, \epsilon_2, s\}$ and eigenvalues $\left\{\Lambda_1^2, \Lambda_2^2\right\}$ follow from

$$0 = \begin{vmatrix} \epsilon_1 - \Lambda^2 & s \\ -s & \epsilon_2 - \Lambda^2 \end{vmatrix} = \Lambda^4 - (\epsilon_1+\epsilon_2)\Lambda^2 + (\epsilon_1\epsilon_2 + s^2), \tag{3.23}$$

with solution

$$\Lambda_{1,2}^2 = \frac{\epsilon_1+\epsilon_2}{2} \pm \sqrt{\frac{(\epsilon_1-\epsilon_2)^2}{4} - s^2}. \tag{3.24}$$

This can be inverted for $\epsilon_{1,2}$ for later use to

$$\epsilon_{1,2} = \frac{\Lambda_1^2 + \Lambda_2^2}{2} \pm \sqrt{\frac{\left(\Lambda_1^2 - \Lambda_2^2\right)^2}{4} + s^2}. \tag{3.25}$$

This immediately leads to

$$\lambda_1 + \lambda_2 = \mathrm{Tr}(CC^T) = \epsilon_1^2 + \epsilon_2^2 + 2s^2 = \Lambda_1^4 + \Lambda_2^4 + 4s^2. \tag{3.26}$$

On inserting equations (3.21) and (3.26) into equation (3.19), we can express $P(C)$ in terms of $\Lambda_{1,2}^2$. However, we have changed variables twice to arrive here, first from the matrix elements c_{ij} of C to $\{\epsilon_1, \epsilon_2, s, \theta\}$ and second from $\{\epsilon_1, \epsilon_2\}$ to $\left\{\Lambda_1^2, \Lambda_2^2\right\}$. The corresponding Jacobians we must multiply by are given by

$$\begin{aligned} \mathcal{J}_1 &= \left|\frac{\partial\{c_{11}, c_{12}, c_{21}, c_{22}\}}{\partial\{\epsilon_1, \epsilon_2, s, \theta\}}\right| = 2|\epsilon_1 - \epsilon_2| \cos^2(2\theta), \\ \mathcal{J}_2 &= \left|\frac{\partial\{\epsilon_1, \epsilon_2\}}{\partial\left\{\Lambda_1^2, \Lambda_2^2\right\}}\right| = \left|\frac{\Lambda_1^2 - \Lambda_2^2}{\epsilon_1 - \epsilon_2}\right|. \end{aligned} \tag{3.27}$$

3.2.1. Distinction of real and complex eigenvalues. In order to give the jpdf from equation (3.19) for variables $\Lambda_{1,2}^2$ alone, we have to integrate over the remaining real variables s and θ. Here we have to distinguish between the case of two real eigenvalues, and that of a complex conjugate pair. Starting from a real matrix C in equation (3.22), all new variables, in particular $\epsilon_{1,2}$, are real. In view of equation (3.25), there are two possibilities if the radicand is to remain positive:

(i) Λ_1^2, Λ_2^2 are both real $\Rightarrow \frac{1}{4}\left(\Lambda_1^2 - \Lambda_2^2\right)^2 + s^2 \geqslant 0$ which is always satisfied, or

(ii) Λ_1^2, Λ_2^2 are complex conjugates: $\Lambda_1^2 - \Lambda_2^2 \in \mathrm{i}\mathbb{R} \Rightarrow s^2 \geqslant -\frac{1}{4}\left(\Lambda_1^2 - \Lambda_2^2\right)^2 \geqslant 0$.

We thus obtain for the jpdf

$$\begin{aligned} \mathrm{d}\Lambda_1^2\, \mathrm{d}\Lambda_2^2 P\left(\Lambda_1^2, \Lambda_2^2\right) = \frac{2c_{N=2}\eta_+}{\pi^{3/2}}\, \mathrm{d}\Lambda_1^2\, \mathrm{d}\Lambda_2^2\, \mathrm{e}^{\eta_-(\Lambda_1^2+\Lambda_2^2)} |\Lambda_1^2\Lambda_2^2|^{\nu/2} \int_0^{2\pi} \mathrm{d}\theta\, \left|\Lambda_1^2 - \Lambda_2^2\right| \cos^2(2\theta) \\ \times \int_{s_{\min}}^{\infty} \mathrm{d}s 2 \int_0^{\infty} \frac{\mathrm{d}t}{\sqrt{t}} \exp\left[-\eta_+^2\left(\Lambda_1^4 + \Lambda_2^4 + 4s^2\right)t - \frac{1}{4t}\right] K_{\frac{\nu}{2}}\left(2\eta_+^2\left|\Lambda_1^2\Lambda_2^2\right|t\right), \end{aligned} \tag{3.28}$$

where $s_{\min}^2 = \max\left\{0, -\left(\Lambda_1^2 - \Lambda_2^2\right)^2/4\right\}$. The θ-integral is trivial.

For two real eigenvalues having $s_{\min} = 0$, the integral over s can be performed, leading to the following simplification for the remaining t-integral:

$$2\int_0^{\infty} \frac{\mathrm{d}t}{t}\, \mathrm{e}^{-\eta_+^2(\Lambda_1^4+\Lambda_2^4)t - \frac{1}{4t}} K_{\frac{\nu}{2}}\left(2\eta_+^2\left|\Lambda_1^2\Lambda_2^2\right|t\right) = 2K_{\frac{\nu}{2}}\left(\eta_+\left|\Lambda_1^2\right|\right) 2K_{\frac{\nu}{2}}\left(\eta_+\left|\Lambda_2^2\right|\right). \tag{3.29}$$

Here we have used equation 6.653.2 of [34] after changing variables $t \to u = \frac{1}{2t}$. When ordering the two eigenvalues as $\Lambda_1^2 > \Lambda_2^2$, the jpdf equation (3.28) can thus be written as

$$P\left(\Lambda_1^2, \Lambda_2^2\right) = c_{N=2}\left(\Lambda_1^2 - \Lambda_2^2\right) \prod_{j=1,2} |\Lambda_j^2|^{\nu/2}\, \mathrm{e}^{\eta_-\Lambda_j^2}\, 2K_{\frac{\nu}{2}}\left(\eta_+\left|\Lambda_j^2\right|\right), \qquad \Lambda_{1,2}^2 \in \mathbb{R}, \tag{3.30}$$

as was claimed in equation (2.9) in conjunction with equation (2.13) for $N = 2$.

For two complex conjugate eigenvalues, the s-integral leads to the complementary error function, without further simplification. Here we order $0 < \mathrm{Im}\Lambda_1^2 = -\mathrm{Im}\Lambda_2^2$ as in equation (2.10) to obtain the following real, positive distribution:

$$P\big(\Lambda_1^2,\Lambda_2^2\big)\,\mathrm{d}\Lambda_1^2\,\mathrm{d}\Lambda_2^2 = c_{N=2}\,\mathrm{d}\Lambda_1^2\,\mathrm{d}\Lambda_2^2\big(\Lambda_1^2-\Lambda_2^2\big)\big|\Lambda_1^2\big|^{\nu/2}|\Lambda_2^2|^{\nu/2}\,\mathrm{e}^{\eta_-(\Lambda_1^2+\Lambda_2^2)} \times 2\int_0^\infty \frac{\mathrm{d}t}{t}\,\mathrm{e}^{-\eta_+^2(\Lambda_1^4+\Lambda_2^4)t-\frac{1}{4t}}\,K_{\frac{\nu}{2}}\big(2\eta_+^2\Lambda_1^2\Lambda_2^2t\big)\mathrm{erfc}\big(\eta_+\sqrt{t}\big|\Lambda_1^2-\Lambda_2^2\big|\big), \quad \Lambda_{1,2}^2\in\mathbb{C}. \tag{3.31}$$

Because the integral depends only on the modulus $|\mathrm{Im}\Lambda_1^2| = |\mathrm{Im}\Lambda_2^2|$, we can define its square root to be the weight of each eigenvalue Λ_j^2, as in equation (2.14). The limit $|\mathrm{Im}\Lambda_1^2| \to 0$ smoothly reduces the integral in equation (3.31) to equation (3.29), using that $\mathrm{erfc}(0) = 1$.

Combining the real and complex cases, and still assuming the eigenvalue ordering, we can write the jpdf most generally as follows:

$$\mathrm{d}^2z_1\,\mathrm{d}^2z_2P(z_1,z_2) = c_{N=2}\,\mathrm{d}^2z_1\,\mathrm{d}^2z_2(z_1-z_2)w(z_1)w(z_2) \times\big(\delta(y_1)\delta(y_2)\Theta(x_1-x_2)-2\mathrm{i}\delta^2(z_1-z_2^*)\Theta(y_1)\big), \tag{3.32}$$

where we have switched variables $\Lambda^2 = z = x+\mathrm{i}y$, including for the differentials, $\mathrm{d}\Lambda^2\,\mathrm{d}\Lambda^{*2} = (\mathrm{d}x+\mathrm{i}\mathrm{d}y)(\mathrm{d}x-\mathrm{i}\mathrm{d}y) = -2\mathrm{i}\mathrm{d}x\,\mathrm{d}y = -2\mathrm{i}\,\mathrm{d}^2z$. This is just the jpdf in equation (2.9) including the weight equation (2.12), and this completes our computation for the $N = 2$ case.

3.3. General structure for arbitrary N

In this subsection, we will compute the jpdf for any N—both even and odd—given in terms of the eigenvalues Λ_j^2 of the Wishart matrix $C = AB^T$. We start from equation (2.7) which we repeat here for convenience:

$$P(C)\sim\exp[\eta_-\,\mathrm{Tr}C]\int_{\mathbb{R}^{N(N+\nu)}}\mathrm{d}A\int_{\mathbb{R}^{N(N+\nu)}}\mathrm{d}B\,\exp\Big[-\frac{\eta_+}{2}\,\mathrm{Tr}(AA^T+BB^T)\Big]\delta(C-AB^T). \tag{3.33}$$

We will eventually use the results from the previous two subsections as building blocks.

Instead of using a generalized Schur (or QZ) decomposition involving unitary matrices to bring A and B to the upper triangular form, we will restrict ourselves here to orthogonal transformations. The best we can achieve in this way is a so-called almost (or quasi) upper triangular (AUT) form for one of the matrices, and an upper triangular form for the second (which is also AUT). An AUT matrix is composed of a block diagonal matrix, having non-vanishing 2×2 blocks along the diagonal for even N, and an additional 1×1 block at the end if N is odd. The remaining non-zero elements of an AUT matrix all lie above the block diagonal.

The precise transformation that we make is

$$A = O_A(\Delta_A+\Lambda_A)O_B^T, \qquad B^T = O_B(\Delta_B+\Lambda_B)O_A^T. \tag{3.34}$$

Here Λ_A and Λ_B are block diagonal, and Δ_A and Δ_B are zero except in elements strictly above the block diagonal. $\Delta_A+\Lambda_A$ and $\Delta_B+\Lambda_B$ are hence AUT. Note that O_A is of size $N\times N$, and O_B is of size $(N+\nu)\times(N+\nu)$. Δ_A and Λ_A are each of the same size as A itself (i.e. rectangular), and similarly Δ_B and Λ_B are of the same size as B^T.

To make the transformation (3.34) unique, having the same number of degrees of freedom (dof) on the left- and right-hand sides, we restrict O_A and O_B as follows:

$$\begin{aligned} &O_A\in O(N)/O(2)^{N/2}, && O_B\in O(N+\nu)/O(2)^{N/2}O(\nu) && \text{for even } N,\\ &O_A\in O(N)/O(2)^{(N-1)/2}, && O_B\in O(N+\nu)/O(2)^{(N-1)/2}O(\nu) && \text{for odd } N. \end{aligned} \tag{3.35}$$

Table 1. Counting dof of matrix $\mathcal{D}$ equation (2.2) before and after change of variables.

Matrix	Degrees of freedom	Matrix	Degrees of freedom	
			Even N	Odd N
A	$N(N+\nu)$	Λ_A	$2N$	$2N-1$
B	$(N+\nu)N$	Λ_B	$2N$	$2N-1$
		Δ_A	$\frac{N^2}{2}-N+\nu N$	$\frac{N^2+1}{2}-N+\nu N$
		Δ_B	$\frac{N^2}{2}-N$	$\frac{N^2+1}{2}-N$
		O_A	$\frac{N^2}{2}-N$	$\frac{N^2+1}{2}-N$
		O_B	$\frac{N^2}{2}-N+\nu N$	$\frac{N^2+1}{2}-N+\nu N$

The residual symmetries leading to these cosets are rotations within each block on the diagonal, and, loosely speaking, the extra factor $O(\nu)$ can be thought of as originating from the reduction of B from the rectangular to the square form, as in the $N=1$ and 2 cases earlier. The precise counting of dof is given in table 1, matching the sum of dof of A and B for all N.

Under this orthogonal transformation, the integrand in equation (2.7) changes as follows:

$$\exp\left[-\frac{\eta_+}{2}\operatorname{Tr}(AA^T+BB^T)\right]=\exp\left[-\frac{\eta_+}{2}\operatorname{Tr}\big(\Lambda_A\Lambda_A^T+\Lambda_B\Lambda_B^T+\Delta_A\Delta_A^T+\Delta_B\Delta_B^T\big)\right]. \quad (3.36)$$

The pre-factor $\exp[\eta_-\operatorname{Tr}C]=\exp\big[\eta_-\sum_{i=1}^N\Lambda_i^2\big]$ remains unchanged, with the relation between the eigenvalues Λ_i^2 and the new variables yet to be determined.

The transformation equation (3.34) leads to the following differentials:

$$\begin{aligned}(\mathrm{d}A)_{ij}&=\big(O_A\big[O_A^T\,\mathrm{d}O_A(\Delta_A+\Lambda_A)-(\Delta_A+\Lambda_A)O_B^T\,\mathrm{d}O_B+\mathrm{d}\Delta_A+\mathrm{d}\Lambda_A\big]O_B^T\big)_{ij},\\(\mathrm{d}B^T)_{ij}&=\big(O_B\big[O_B^T\,\mathrm{d}O_B(\Delta_B+\Lambda_B)-(\Delta_B+\Lambda_B)O_A^T\,\mathrm{d}O_A+\mathrm{d}\Delta_B+\mathrm{d}\Lambda_B\big]O_A^T\big)_{ij}.\end{aligned} \quad (3.37)$$

Here we have used the fact that for orthogonal transformations (with $O^TO=I$), the differential $O^T\,\mathrm{d}O$ is anti-symmetric. This remains true for our special choice of cosets. When considering the invariant line element $\operatorname{Tr}(\mathrm{d}A\,\mathrm{d}A^T+\mathrm{d}B\,\mathrm{d}B^T)$, the rotations outside the square brackets in equation (3.37) can be dropped.

We will now compute the Jacobian for the change of variables from $\{\mathrm{d}A,\mathrm{d}B^T\}$ to $\big\{\mathrm{d}\Lambda_A,\mathrm{d}\Lambda_B,\mathrm{d}\Delta_A,\mathrm{d}\Delta_B,O_A^T\mathrm{d}O_A,O_B^T\,\mathrm{d}O_B\big\}$. Here we use the differentials for convenience as for the orthogonal matrices, only these constitute independent variables (see also [31] for a similar discussion for the real Ginibre ensemble). In particular, counting dof $O_A^T\,\mathrm{d}O_A$ is an anti-symmetric matrix with zeros not just on the diagonal but on the block diagonal. Similarly $O_B^T\,\mathrm{d}O_B$ is an anti-symmetric matrix with zeros on the block diagonal for the first N elements, and a zero-block of size $\nu\times\nu$ on the remaining part of the diagonal.

In the differential equation (3.37), the variables $\{\mathrm{d}\Lambda_A,\mathrm{d}\Lambda_B,\mathrm{d}\Delta_A,\mathrm{d}\Delta_B\}$ are already diagonal, with

$$\frac{\partial(\mathrm{d}A)_{ij}}{\partial(\mathrm{d}\Delta_A)_{pq}}=\delta_{ip}\delta_{jq},\qquad\frac{\partial(\mathrm{d}A)_{ij}}{\partial(\mathrm{d}\Lambda_A)_{pq}}=\delta_{ip}\delta_{jq}, \quad (3.38)$$

and similarly for $\mathrm{d}B^T$. This contributes a unity matrix block to the Jacobi matrix $\mathcal{J}$, when considering the corresponding elements of $\{\mathrm{d}A,\mathrm{d}B^T\}$ on and above the block diagonal.

The non-trivial contribution from the Jacobian therefore originates from differentiating the remaining elements of $\{\mathrm{d}A,\mathrm{d}B^T\}$ below the block diagonal with respect to the independent variables of $\big\{O_A^T\,\mathrm{d}O_A,O_B^T\,\mathrm{d}O_B\big\}$, where we also choose the lower block diagonal elements for convenience. When appropriately ordering the elements of the Jacobi matrix (see appendix A

and also a similar discussion in [31]), the contributions proportional to Δ_A and Δ_B in equation (3.37) will drop out, being part of a lower triangular sub-matrix in $\mathcal{J}$.

For the sake of argument, we restrict ourselves in this section to the case of Λ_A and Λ_B being diagonal. The more general (and typical) case in which Λ_A and Λ_B contain 2×2 blocks is treated in appendix A.

Arranging the remaining matrix elements below the block diagonal of $\mathrm{d}A$ and of the square part of $\mathrm{d}B^T$ into pairs, this leads to a 2×2 block diagonal Jacobi sub-matrix with elements

$$\left|\det\begin{pmatrix} \frac{\partial(\mathrm{d}A)_{ij}}{\partial(O_A^T dO_A)_{ij}} & \frac{\partial(\mathrm{d}B)_{ij}}{\partial(O_A^T dO_A)_{ij}} \\ \frac{\partial(\mathrm{d}A)_{ij}}{\partial(O_B^T dO_B)_{ij}} & \frac{\partial(\mathrm{d}B)_{ij}}{\partial(O_B^T dO_B)_{ij}} \end{pmatrix}\right| = \left|\det\begin{pmatrix} (\Lambda_A)_{jj} & -(\Lambda_B)_{ii} \\ -(\Lambda_A)_{ii} & (\Lambda_B)_{jj} \end{pmatrix}\right| = \left|\Lambda_j^2-\Lambda_i^2\right|, \tag{3.39}$$

where we used that $(\Lambda_A)_{jj}(\Lambda_B)_{jj}=\Lambda_j^2$ (no summations), and the Λ_j^2 are the eigenvalues of the matrix $C\equiv AB^T$. The remaining νN matrix elements below the block diagonal of $\mathrm{d}B^T$ give a diagonal sub-matrix with ν elements $(\Lambda_B)_{jj}$ each. The resulting contribution to the Jacobian is

$$\mathcal{J}=\prod_{1\leqslant i<j\leqslant N}{}' \left|\Lambda_i^2-\Lambda_j^2\right| \prod_{j=1}^{N}|(\Lambda_B)_{jj}|^{\nu}. \tag{3.40}$$

The prime on the product symbol denotes that only those factors with indices (i,j) strictly below the block diagonal are to be included. Finally, we observe that the second product can be written as

$$\prod_{j=1}^{N}|(\Lambda_B)_{jj}|^{\nu}=\begin{cases}\displaystyle\prod_{j=1}^{N/2}|\det B_j|^{\nu} & \text{for even } N,\\ \displaystyle\prod_{j=1}^{(N-1)/2}|\det B_j|^{\nu}|(\Lambda_B)_{NN}|^{\nu} & \text{for odd } N,\end{cases} \tag{3.41}$$

in which B_j is the jth 2×2 block along the diagonal of the matrix Λ_B. The same statement is true in the more general case when Λ_A (and Λ_B) is not diagonal, as shown in appendix A.

Writing everything together, we have for the total measure

$$\begin{aligned}&\mathrm{d}A\,\mathrm{d}B\,\mathrm{e}^{\eta_-\operatorname{Tr}AB^T-\frac{\eta_+}{2}\operatorname{Tr}(AA^T+BB^T)}\\ &\sim \mathrm{d}\Lambda_A\,\mathrm{d}\Lambda_B\,\mathrm{d}\Delta_A\,\mathrm{d}\Delta_B\,O_A^{-1}\,\mathrm{d}O_A\,O_B^{-1}\,\mathrm{d}O_B\prod_{1\leqslant i<j\leqslant N}{}'\left|\Lambda_i^2-\Lambda_j^2\right|\prod_{i=1}^{N}\mathrm{e}^{\eta_-\Lambda_i^2}\\ &\times\mathrm{e}^{-\frac{\eta_+}{2}\operatorname{Tr}(\Lambda_A^T\Lambda_A+\Lambda_B^T\Lambda_B+\Delta_A^T\Delta_A+\Delta_B^T\Delta_B)}\begin{cases}\displaystyle\prod_{j=1}^{N/2}|\det B_j|^{\nu} & \text{for even } N\\ \displaystyle\prod_{j=1}^{(N-1)/2}|\det B_j|^{\nu}|\Lambda_B|_{NN}^{\nu} & \text{for odd } N.\end{cases}\end{aligned} \tag{3.42}$$

All constant factors are omitted here; we give the overall normalization constant later. We reiterate that B_j here is the jth 2×2 block on the diagonal of Λ_B. The integration over the orthogonal dof as well as over the upper block triangular matrices $\Delta_{A,B}$ can now be performed as they decouple. The relevant dof for the right-hand side of equation (3.42) can thus be

written in terms of the Λ_i^2 and 2×2 blocks of the matrices $\Lambda_{A,B}$:

$$\prod_{i<j}{}' \left|\Lambda_i^2-\Lambda_j^2\right| \begin{cases} \displaystyle\prod_{i=1}^{N/2}\left\{\mathrm{d}A_i\,\mathrm{d}B_i\,\mathrm{e}^{\eta_-(\Lambda_{2i-1}^2+\Lambda_{2i}^2)}\,\mathrm{e}^{-\frac{\eta_+}{2}\mathrm{Tr}(A_i^TA_i+B_i^TB_i)}|\det B_i|^\nu\right\} & \text{for even } N,\\ \displaystyle\prod_{i=1}^{(N-1)/2}\left\{\mathrm{d}A_i\,\mathrm{d}B_i\,\mathrm{e}^{\eta_-(\Lambda_{2i-1}^2+\Lambda_{2i}^2)}\,\mathrm{e}^{-\frac{\eta_+}{2}\mathrm{Tr}(A_i^TA_i+B_i^TB_i)}|\det B_i|^\nu\right\} & \\ \quad\times \mathrm{d}a\,\mathrm{d}b\,\mathrm{e}^{\eta_-\Lambda_N^2}\,\mathrm{e}^{-\frac{\eta_+}{2}(a^2+b^2)}|b|^\nu & \text{for odd } N. \end{cases} \tag{3.43}$$

We have thus reduced the problem of computing the jpdf to a simpler problem involving only 2×2 and 1×1 blocks, which can be handled just as the $N=2$ and $N=1$ cases that we treated in the previous two subsections. For this, it is necessary to order the eigenvalues as described in equation (2.10). Then, following equation (3.32), each 2×2 block will make the following contribution in variables $\Lambda_i^2=z_i$ (with Λ_{2i-1}^2 and Λ_{2i}^2 either both real or complex conjugates, and ordered as described at the end of section 3.2):

$$\begin{aligned}&\mathrm{d}^2z_{2i-1}\,\mathrm{d}^2z_{2i}(z_{2i-1}-z_{2i})w(z_{2i-1})w(z_{2i})\\ &\qquad\times(\delta(y_{2i-1})\delta(y_{2i})\Theta(x_{2i-1}-x_{2i})-2i\delta^2(z_{2i-1}-z_{2i}^*)\Theta(y_{2i-1})).\end{aligned} \tag{3.44}$$

In a similar way, we have for the 1×1 block when N is odd

$$\mathrm{d}^2z_N|z_N|^{\nu/2}\,\mathrm{e}^{\eta_-z_N}g(z_N)\delta(y_N)=\mathrm{d}^2z_N\,w(z_N)\delta(y_N), \tag{3.45}$$

where z_N will be real. Note that collecting all these quantities in equation (3.43) for each $i=1$ to $[N/2]$, the factors $\Lambda_{2i-1}^2-\Lambda_{2i}^2$ will combine with the $\prod_{i<j}{}'(\Lambda_i^2-\Lambda_j^2)$ to make a true Vandermonde determinant $\prod_{i<j}(\Lambda_i^2-\Lambda_j^2)$, and we were able to drop the modulus sign because of the chosen ordering. The final answer for the jpdf is therefore as claimed in equation (2.9). The normalization constant can be determined by keeping track of all volume factors and μ-dependences; it is given by

$$c_N=(\mathrm{VO}(N)2^{-N}(2\pi)^{-N(N+1)/4})^2(2\pi)^{-N\nu/2}\frac{\mathrm{VO}(N+\nu)}{\mathrm{VO}(N)\mathrm{VO}(\nu)}(2\mu)^{-N(N+\nu)}\eta_+^{-N(N+\nu-1)/2}. \tag{3.46}$$

4. Finite- and large-N density correlation functions

4.1. The kernel

The kernel $\mathcal{K}_N(z_1,z_2)$ as it initially appears in equation (2.18) is *defined* as follows [7]:

$$\mathcal{K}_N(z_1,z_2)\equiv\sum_{k=1}^{N}\sum_{l=1}^{N}\mathcal{A}_{kl}^{-1}z_1^{k-1}z_2^{l-1}, \tag{4.1}$$

where the matrix $\mathcal{A}$ of dressed moments is related to $\mathcal{F}$ by

$$\mathcal{A}_{kl}\equiv\int\mathrm{d}^2z_1\,\mathrm{d}^2z_2\mathcal{F}(z_1,z_2)z_1^{k-1}z_2^{l-1}. \tag{4.2}$$

However, to evaluate the matrix $\mathcal{A}$ and its inverse directly is not trivial in general. Fortunately, the kernel may also be derived from the expectation value of the product of two characteristic polynomials [20]:

$$H_N(\lambda,\gamma)\equiv\langle\det(\lambda-\mathcal{D})\det(\gamma-\mathcal{D}^T)\rangle_N, \tag{4.3}$$

where $\mathcal{D}$ was given in equation (2.2). An explicit form for $H_N(\lambda, \gamma)$ was derived by the authors in [20][7]. In the case of the real Ginibre ensemble, the spectral density was known prior to its integrability [4] and thus was used for the determination of the kernel in [7].

To establish the relationship between $\mathcal{K}_N(z_1, z_2)$ and $H_{N-2}(\lambda, \gamma)$, we first relate the latter to the complex eigenvalue density $R^{\mathbb{C}}_{1,N}(z)$. If we choose $\gamma = \lambda^*$ with $\mathrm{Im}\,\lambda^2 > \mathrm{Im}\,\gamma^2$, we have

$$\begin{aligned} H_{N-2}(\lambda, \lambda^*) &= \int_{\mathbb{C}} \mathrm{d}^2 z_1 \ldots \int_{\mathbb{C}} \mathrm{d}^2 z_{N-2} P_{N-2}(z_1, \ldots, z_{N-2})(\lambda\lambda^*)^\nu \prod_{j=1}^{N-2} (\lambda^2 - z_j)(\lambda^{*2} - z_j) \\ &= \frac{c_{N-2}}{c_N} \frac{1}{\exp[-\eta_-(\lambda^2 + \lambda^{2*})] g(\lambda^2)^2 (\lambda^2 - \lambda^{2*})(-2\mathrm{i})\Theta(\mathrm{Im}\,\lambda^2)} \\ &\quad \times \int_{\mathbb{C}} \mathrm{d}^2 z_1 \ldots \int_{\mathbb{C}} \mathrm{d}^2 z_{N-2} \tilde{P}_N(z_1, \ldots, z_{N-2}, \lambda^2, \lambda^{2*}), \end{aligned} \tag{4.4}$$

where $\tilde{P}_N$ indicates that this jpdf is conditioned that the last two eigenvalues are complex conjugates and ordered. The last line in equation (4.4) is thus nothing but the complex density $R^{\mathbb{C}}_{1,N}(\lambda^2)$, obtained by inserting a delta function into the partition function together with the constraint that the last two eigenvalues are complex conjugates. We thus arrive at the following relationship:

$$R^{\mathbb{C}}_{1,N}(z) = \frac{c_N}{c_{N-2}} \frac{w(z)w(z^*)}{|z|^\nu} (-2\mathrm{i})(z - z^*) H_{N-2}(\sqrt{z}, \sqrt{z^*}). \tag{4.5}$$

On the other hand, we have from equation (2.25) an equation that relates the complex density directly to the kernel

$$R_{1,N}(z) = \int_{\mathbb{C}} \mathrm{d}^2 u \mathcal{K}_N(z, u) \mathcal{F}(u, z) \tag{4.6}$$

and so for the complex z inserting equation (2.19)

$$R^{\mathbb{C}}_{1,N}(z) = \mathcal{K}_N(z, z^*) w(z) w(z^*)(-2\mathrm{i})\ \mathrm{sgn}(y). \tag{4.7}$$

We can therefore make the identification (after analytic continuation in each argument)

$$\mathcal{K}_N(u, v) = \frac{c_N}{c_{N-2}} (u - v) \frac{H_{N-2}(\sqrt{u}, \sqrt{v})}{(uv)^{\nu/2}}. \tag{4.8}$$

Using the solution for $H_N(\lambda, \gamma)$ obtained in [20] as well as equation (3.46), we then have for the properly normalized kernel that

$$\begin{aligned} \mathcal{K}_N(u, v) = \frac{\eta_-}{8\pi(4\mu^2\eta_+)^{\nu+1}} \sum_{j=0}^{N-2} \left(\frac{\eta_-}{\eta_+}\right)^{2j} \frac{(j+1)!}{(j+\nu)!} \Bigg\{ L^\nu_{j+1}\left(\frac{v}{4\mu^2\eta_-}\right) L^\nu_j\left(\frac{u}{4\mu^2\eta_-}\right) \\ - L^\nu_{j+1}\left(\frac{u}{4\mu^2\eta_-}\right) L^\nu_j\left(\frac{v}{4\mu^2\eta_-}\right) \Bigg\}, \end{aligned} \tag{4.9}$$

which is the same as equation (2.20). It can be further simplified to be expressed as an anti-symmetric derivative as follows. For modified Laguerre polynomials, we can use a recurrence relation to show that

$$\begin{aligned} (j+1)\left\{L^\nu_{j+1}(y)L^\nu_j(x) - (x \leftrightarrow y)\right\} &= \left(y\frac{\partial}{\partial y} L^\nu_j(y) + (j + \nu + 1 - y) L^\nu_j(y)\right) L^\nu_j(x) - (x \leftrightarrow y) \\ &= \left(y\frac{\partial}{\partial y} - x\frac{\partial}{\partial x} - (y - x)\right) L^\nu_j(x) L^\nu_j(y). \end{aligned} \tag{4.10}$$

[7] Note that P and Q were called A and B in [20]; we set n in [20] to unity here.

The kernel therefore becomes

$$\mathcal{K}_N(z_1,z_2)=\frac{\eta_-}{8\pi(4\mu^2\eta_+)^{\nu+1}}\left(y\frac{\partial}{\partial y}-x\frac{\partial}{\partial x}-(y-x)\right)\sum_{j=0}^{N-2}\left(\frac{\eta_-}{\eta_+}\right)^{2j}\frac{j!}{(j+\nu)!}L_j^\nu(x)L_j^\nu(y), \tag{4.11}$$

where x and y are evaluated at $x=z_1/4\mu^2\eta_-$ and $y=z_2/4\mu^2\eta_-$ after the differentiations. The symmetric kernel in terms of Laguerre polynomials on the right-hand side of equation (4.11) is nothing else but the kernel of the complex ($\beta=2$) two-matrix model [16].

We have explicitly checked that a similar relation holds relating the kernel of the non-chiral real Ginibre ensemble (see the equation after 5.26 in the second reference of [8]) to $(\partial_y-\partial_x-2(y-x))$ operating on the kernel of the non-chiral complex Ginibre ensemble (see equation (40) in [32]) and thus this is a more general feature.

Note that the convention used in [20] for defining the 'kernel' was different from that adopted here (in equation (4.9)); in that paper, there was no division by $(uv)^{\nu/2}$ and the summation ran to N. There was also a minor typographical error in the arguments of one function (equation (33) in [20]).

4.2. Finite-N results

From equation (2.18), we have

$$R_1(z_1)=\int_{\mathbb{C}}\mathrm{d}^2z\mathcal{K}_N(z_1,z)\mathcal{F}(z,z_1)\equiv R_1^{\mathbb{C}}(z_1)+\delta(y_1)R_1^{\mathbb{R}}(x_1). \tag{4.12}$$

We now simply insert the finite-N kernel equation (4.9) and weight function equation (2.12) into this using equation (2.19), to give

$$\begin{aligned}R_1^{\mathbb{C}}(z)=&-2\mathrm{i}\,\mathrm{sgn}(\mathrm{Im}\,z)\,2\int_0^\infty\frac{\mathrm{d}t}{t}\,\mathrm{e}^{-\eta_+^2t(z^2+z^{*2})-\frac{1}{4t}}K_{\frac{\nu}{2}}\left(2\eta_+^2t|z|^2\right)\mathrm{erfc}(2\eta_+\sqrt{t}|\mathrm{Im}\,z|)\\&\times\frac{\eta_-|z|^\nu\,\mathrm{e}^{2\eta_-\mathrm{Re}\,z}}{8\pi(4\mu^2\eta_+)^{\nu+1}}\sum_{j=0}^{N-2}\left(\frac{\eta_-}{\eta_+}\right)^{2j}\frac{(j+1)!}{(j+\nu)!}\left\{L_{j+1}^\nu\left(\frac{z^*}{4\mu^2\eta_-}\right)L_j^\nu\left(\frac{z}{4\mu^2\eta_-}\right)-\mathrm{c.c.}\right\}\end{aligned} \tag{4.13}$$

$$\begin{aligned}R_1^{\mathbb{R}}(x)=&\frac{\eta_-}{8\pi(4\mu^2\eta_+)^{\nu+1}}\int_{-\infty}^\infty\mathrm{d}x'\mathrm{sgn}(x-x')|xx'|^{\nu/2}\,\mathrm{e}^{\eta_-(x+x')}2K_{\frac{\nu}{2}}(\eta_+|x|)2K_{\frac{\nu}{2}}(\eta_+|x'|)\\&\times\sum_{j=0}^{N-2}\left(\frac{\eta_-}{\eta_+}\right)^{2j}\frac{(j+1)!}{(j+\nu)!}\left\{L_{j+1}^\nu\left(\frac{x'}{4\mu^2\eta_-}\right)L_j^\nu\left(\frac{x}{4\mu^2\eta_-}\right)-(x'\leftrightarrow x)\right\}.\end{aligned} \tag{4.14}$$

These results are valid for even N only. Alternatively, we could have used the form of equation (4.11) which is more reminiscent of the corresponding chGOE result [35] at $\mu=0$. In fact we have checked that in the limit $\mu\to 0$, the complex density equation (4.13) vanishes, and the real density equation (4.14) reduces to the finite-N expression (equation (5.18) in [35]) for the chGOE, after using some identities for modified Laguerre polynomials. We have also checked these results numerically using Monte Carlo, by generating random matrices and explicitly diagonalizing them.

As the last step we can change from squared variables $z=x+\mathrm{i}y=\Lambda^2$ to Dirac eigenvalues Λ, using equation (2.28). These two densities are illustrated[8] in figures 1 and 2, showing the localization of the support for finite N.

[8] Here and in the following, numerical integrals are carried out using [36].

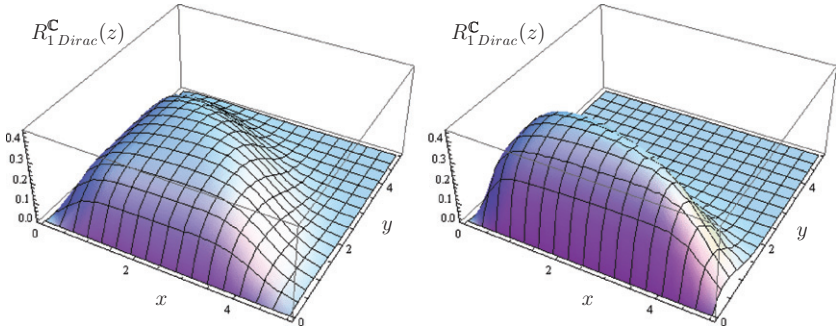

Figure 1. The complex spectral density $R^{\mathbb{C}}_{1\,\mathrm{Dirac}}(z)$ for finite $N = 10$ at maximal non-Hermiticity $\mu^2 = 1$ (left) and intermediate $\mu^2 = 0.5$ (right), both for $\nu = 0$. We show only the first quadrant for symmetry reasons. For $\mu = 1$, we see a circular 'support' growing with $\sqrt{N}$, apart from the repulsion from the axes. For decreasing μ, the 'support' becomes an ellipse, with the eigenvalues moving towards, as well as onto, the real axis. Note the increased height in the right plot.

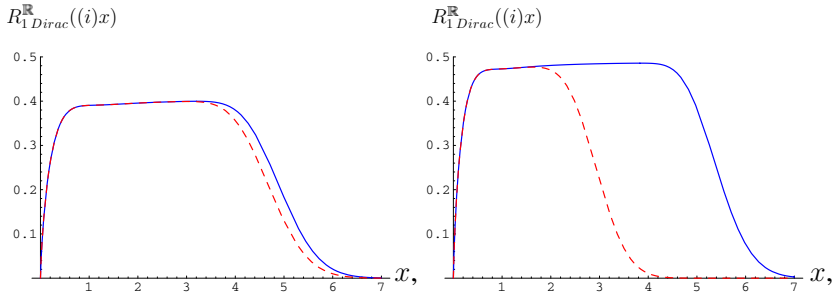

Figure 2. The spectral density $R^{\mathbb{R}}_{1\,\mathrm{Dirac}}(x)$ for real eigenvalues (blue full line) and $R^{\mathbb{R}}_{1\,\mathrm{Dirac}}(\mathrm{i}x)$ for purely imaginary eigenvalues (red dashed line) for finite $N = 10$ at almost maximal non-Hermiticity $\mu^2 = 0.95$ (left) and intermediate $\mu^2 = 0.5$ (right), both for $\nu = 0$. Here we have chosen (almost) the same parameter values as those in figure 1, with $\mu^2 = 0.95$ here close to 1 there. Because of chiral symmetry, real and imaginary eigenvalues come in $\pm$ pairs and we only have to show the positive axes, comparing both distributions in the same plot. Whilst for $\mu^2 = 0.95$, the distributions of real and imaginary Dirac eigenvalues are almost the same, for $\mu^2 = 0.5$ there are more eigenvalues on the real than on the imaginary axis.

4.3. The large-N limit at strong non-Hermiticity

In the strong non-Hermitian limit, we keep μ fixed as we take the large-N limit. This necessitates *no* rescaling of the eigenvalues (see section 2), which is why our result is also true away from the origin. Let us first determine the large-N limit of the kernel.

Equation 8.976.1 in [34] gives us the so-called Hille–Hardy formula (the equivalent of Mehler's formula for Hermite polynomials):

$$S(x,y,z) \equiv \sum_{j=0}^{\infty} \frac{j!}{(j+\nu)!} L_j^{\nu}(x) L_j^{\nu}(y) z^j = \frac{(xyz)^{-\nu/2}}{1-z}\, \mathrm{e}^{-\frac{z}{1-z}(x+y)} I_{\nu}\left(\frac{2\sqrt{xyz}}{1-z}\right). \tag{4.15}$$

We can insert this into equation (4.11) and evaluate it after extending the sum to infinity. On differentiating the right-hand side, certain terms cancel, and we can therefore establish that

$$y\frac{\partial S(x,y,z)}{\partial y} - x\frac{\partial S(x,y,z)}{\partial x} = -\frac{z}{1-z}(y-x)S(x,y,z). \tag{4.16}$$

Hence the limit as $N \to \infty$ of the kernel is easily seen to be

$$\mathcal{K}_\nu^S(z_1, z_2) \equiv \lim_{N\to\infty} \mathcal{K}_N(z_1, z_2) = \frac{\eta_+^3}{8\pi}(z_1 - z_2)\, \mathrm{e}^{-\eta_-(z_1+z_2)}(z_1 z_2)^{-\nu/2} I_\nu(2\eta_+\sqrt{z_1 z_2}). \tag{4.17}$$

Because of this simplification, this is now *proportional* to the $\beta = 2$ kernel at strong non-Hermiticity. Multiplication by the weight function equation (2.12) which contains the modulus $|z_1 z_2|^{\nu/2}$ will only cancel the pre-factor in equation (4.17) up to a phase. Putting all ingredients together, we can determine the eigenvalue densities using equation (2.25):

$$\rho_\nu^{\mathbb{C}S}(z) = \mathrm{sgn}(\mathrm{Im}\, z)(-2\mathrm{i})(z - z^*)\frac{\eta_+^3}{8\pi} I_\nu\,(2\eta_+|z|)$$
$$\times\, 2\int_0^\infty \frac{\mathrm{d}t}{t} \exp\left[-\eta_+^2(z^2 + z^{*2})t - \frac{1}{4t}\right] K_{\frac{\nu}{2}}\left(2\eta_+^2|z|^2 t\right)\mathrm{erfc}(2\eta_+\sqrt{t}|\mathrm{Im}\, z|), \tag{4.18}$$

$$\rho_\nu^{\mathbb{R}S}(x) = \frac{\eta_+^3}{8\pi} 2K_{\frac{\nu}{2}}(\eta_+|x|)\left(\int_0^\infty \mathrm{d}x'|x - x'|\; 2K_{\frac{\nu}{2}}(\eta_+|x'|)\; I_\nu(2\eta_+\sqrt{xx'})\right.$$
$$\left. + \int_{-\infty}^0 \mathrm{d}x'|x - x'|\; 2K_{\frac{\nu}{2}}(\eta_+|x'|)\; J_\nu(2\eta_+\sqrt{x|x'|})\right). \tag{4.19}$$

Note the change from Bessel-*I* to Bessel-*J* function inside the integral for negative arguments, after taking into account the aforementioned phase.

If we rescale the eigenvalues as $2\eta_+ z^2 \to z^2$ (and divide the densities by $2\eta_+$ accordingly), we obtain the same densities as at maximal non-Hermiticity. These are obtained by setting $\mu = 1 \Rightarrow \eta_+ = \frac{1}{2}$ above, or by starting from the kernel equation (2.30) at maximal non-Hermiticity. This feature that the strong limit can be obtained by rescaling the case of maximal non-Hermiticity is generically true for complex RMT, see [30].

In figures 3 and 4, we show the densities of Dirac eigenvalues Λ for complex eigenvalues and real or purely imaginary eigenvalues, respectively, using the mapping equation (2.28). Because of the rescaling property just mentioned, we only show results here for maximal non-Hermiticity. One can check analytically using a saddle-point approximation including the fluctuations that for asymptotically large x, y the density equations (4.18) and (4.19) decay as $\sim 1/|z|$ and $1/\sqrt{x}$, respectively. After the mapping to Dirac eigenvalue equation (2.28) they thus reach a plateau as seen in the figures. We note that the profiles of the densities on the real and imaginary axis are very reminiscent to parallel cuts through the complex densities, for both values of ν shown.

4.4. The large-N limit at weak non-Hermiticity

In the weak case, we scale μ and z with N as follows (as compared with the unscaled case, i.e. we implicitly include here the first rescaling discussed in section 2.4):

$$\mu \equiv \frac{\alpha}{\sqrt{2N}}, \qquad 4Nz \equiv \hat{z}, \tag{4.20}$$

where α and $\hat{z}$ are kept fixed throughout. Because of the rescaling of the eigenvalues here we are magnifying the region around the origin.

For the weight function we thus simply obtain

$$\lim_{N\to\infty} K_{\frac{\nu}{2}}\left(\eta_+\frac{|z|}{4N}\right) = K_{\frac{\nu}{2}}\left(\frac{|z|}{8\alpha^2}\right) \quad \text{and} \quad \lim_{N\to\infty} \exp\left[\eta_-\frac{z}{4N}\right] = \exp\left[\frac{z}{8\alpha^2}\right]. \tag{4.21}$$

For the kernel we are interested in the limit of equation (4.9) in terms of the rescaled variables, i.e. μ, η_- and η_+ which all now depend on N. Instead of using equation (4.11) it is slightly

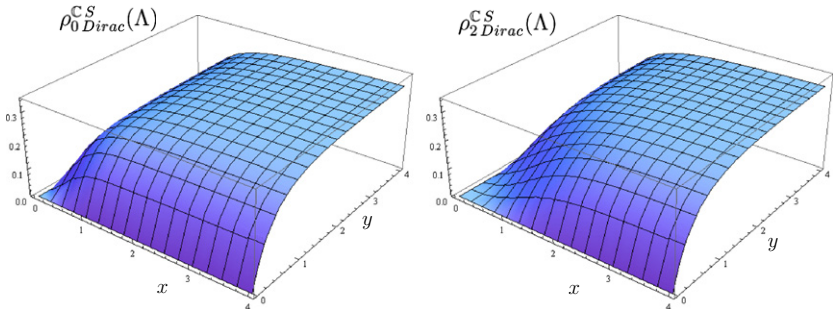

Figure 3. The complex spectral density $\rho^{\mathbb{C}\,S}_{\nu\,\mathrm{Dirac}}(\Lambda = x + \mathrm{i}y)$ at maximal non-Hermiticity $\mu = 1$. It is shown only in the first quadrant for symmetry reasons, for $\nu = 0$ (left) and $\nu = 2$ (right). Increasing the number of exact zero eigenvalues ν leads to a stronger repulsion from the origin. At $\nu = 0$ this repulsion is still present due to chiral symmetry (or technically speaking the presence of the Bessel-K function).

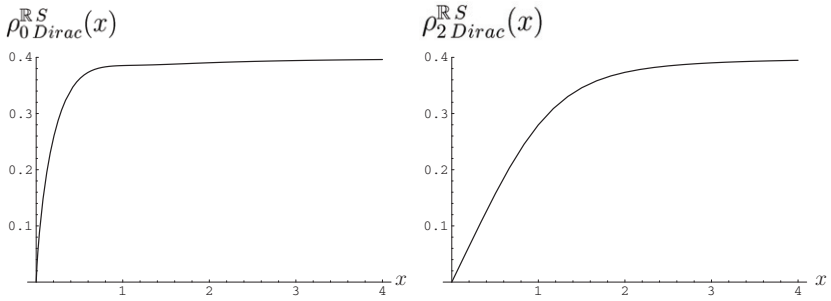

Figure 4. The real spectral density of Dirac eigenvalues on the positive half-line at maximal non-Hermiticity $\mu = 1$ for $\nu = 0$ (left) and $\nu = 2$ (right). Because of chiral symmetry it is symmetric on the negative real line, and because $\mu = 1$ it is identical on the imaginary axis. For $\nu = 2$ we see the increased repulsion from the origin compared to $\nu = 0$, as for the complex eigenvalues in figure 3.

simpler if we can rewrite equation (4.9) so that the Laguerre polynomials inside the sum are of the same degree j. Using the recurrence relationship for the Laguerre polynomials (equation 8.971.2 in [34]), we have

$$(n+1)\left\{L^{\nu}_{n+1}(v)L^{\nu}_{n}(u) - (u \leftrightarrow v)\right\} = \left((n+1+\nu)L^{\nu}_{n}(v) - vL^{\nu+1}_{n}(v)\right)L^{\nu}_{n}(u) - (u \leftrightarrow v)$$
$$= uL^{\nu+1}_{n}(u)L^{\nu}_{n}(v) - vL^{\nu+1}_{n}(v)L^{\nu}_{n}(u). \tag{4.22}$$

The kernel can therefore be written as

$$\mathcal{K}_N(z_1, z_2) = \frac{1}{8\pi(4\mu^2\eta_+)^{\nu+1}4\mu^2}\sum_{j=0}^{N-2}\left(\frac{\eta_-}{\eta_+}\right)^{2j}\frac{j!}{(j+\nu)!}$$
$$\times\left\{z_1 L^{\nu+1}_{j}\left(\frac{z_1}{4\mu^2\eta_-}\right)L^{\nu}_{j}\left(\frac{z_2}{4\mu^2\eta_-}\right) - z_2 L^{\nu+1}_{j}\left(\frac{z_2}{4\mu^2\eta_-}\right)L^{\nu}_{j}\left(\frac{z_1}{4\mu^2\eta_-}\right)\right\}.$$

We now wish to take the limit $N \to \infty$. For this to exist, we must multiply the kernel by the spacing as well as by the appropriate number of zero-eigenvalues from the weight, as given in equation (4.27) below. In equation (4.23) we will replace the sum with an integral over the variable $t \equiv \frac{j}{N} \in [0, 1]$. Because of the different scaling in the weak limit we cannot use the Hille–Hardy formula as before.

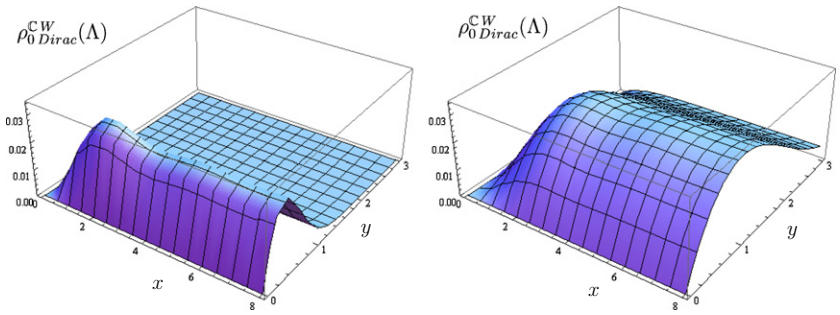

Figure 5. The complex spectral density $\rho^{\mathbb{C}W}_{\nu\ \mathrm{Dirac}}(\Lambda = x + \mathrm{i}y)$ at weak non-Hermiticity for parameters $\alpha^2 = 0.2$ (left) and $\alpha^2 = 1$ (right), both at $\nu = 0$ plotted on the same scale. For increasing α more complex eigenvalues move in towards the imaginary axis, reaching figure 3 left in the limit $\alpha \to \infty$.

In detail, using equation 8.978.2 in [34], we have for some real constant ν and fixed $t \in [0, 1]$ the standard Bessel asymptotic of the modified Laguerre polynomials:

$$\lim_{N\to\infty}\left[N^{-\nu}L^{\nu}_{tN}\left(\frac{x}{N}\right)\right] = t^{\nu/2}x^{-\nu/2}J_{\nu}(2\sqrt{xt}). \tag{4.24}$$

We also have (keeping t fixed so that $j = tN \to \infty$)

$$\lim_{N\to\infty}\left(\frac{1-\frac{\alpha^2}{2N}}{1+\frac{\alpha^2}{2N}}\right)^{2j} = \exp[-2\alpha^2 t] \qquad \text{and} \qquad \lim_{N\to\infty}\frac{j!}{(j+\nu)!}N^{\nu} = t^{-\nu}. \tag{4.25}$$

Therefore,

$$\mathcal{K}^{W}(z_1, z_2) \equiv \lim_{N\to\infty}\left[\frac{1}{(4N)^2}\left(\frac{z_1 z_2}{(4N)^2}\right)^{\nu/2}\mathcal{K}_N\left(\frac{z_1}{4N}, \frac{z_2}{4N}; \mu = \frac{\alpha}{\sqrt{2N}}\right)\right] \tag{4.26}$$

$$= \frac{1}{256\pi\alpha^2}\int_0^1 \mathrm{d}s\, s^2\, \mathrm{e}^{-2\alpha^2 s^2}\{\sqrt{z_1}J_{\nu+1}(s\sqrt{z_1})J_{\nu}(s\sqrt{z_2}) - (z_1 \leftrightarrow z_2)\}$$

$$= \frac{1}{128\pi\alpha^2}\left(z_2\frac{\partial}{\partial z_2} - z_1\frac{\partial}{\partial z_1}\right)\int_0^1 \mathrm{d}s\, s\, \mathrm{e}^{-2\alpha^2 s^2}J_{\nu}(s\sqrt{z_1})J_{\nu}(s\sqrt{z_2}), \tag{4.27}$$

after a simple change of variables in the integral. In the last line we expressed the kernel as a derivative of the $\beta = 2$ kernel at weak non-Hermiticity. This corresponds to equation (4.11) in which the second term $-(y - x)$ now becomes sub-leading compared with the derivatives. The same relation between the large-N kernel at weak non-Hermiticity is true for the $\beta = 1$ and $\beta = 2$ Ginibre ensembles [8, 32], respectively.

Collecting all elements we have for the complex density

$$\rho^{\mathbb{C}W}_{\nu}(z) = -2\mathrm{i}\,\mathrm{sgn}(\mathrm{Im}\,z)\exp\left[\frac{1}{8\alpha^2}2\mathrm{Re}\,z\right]\mathcal{K}^{W}(z, z^*)$$
$$\times\, 2\int_0^{\infty}\frac{\mathrm{d}t}{t}\exp\left[-\frac{t}{64\alpha^4}(z^2 + z^{*2}) - \frac{1}{4t}\right]K_{\frac{\nu}{2}}\left(\frac{t}{32\alpha^4}|z|^2\right)\mathrm{erfc}\left(\frac{\sqrt{t}}{4\alpha^2}|\mathrm{Im}\,z|\right). \tag{4.28}$$

In figure 5, it is shown after mapping to Dirac eigenvalues. As a consistency check we can take the limit $\alpha \to \infty$ while keeping z/α^2 fixed to obtain once more the complex density in the strong non-Hermiticity limit, equation (4.18). The precise mapping of weak

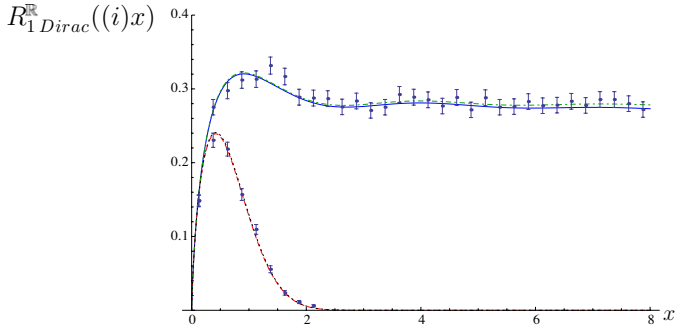

Figure 6. The real spectral density of Dirac eigenvalues on the positive half-line scaled as for weak non-Hermiticity for $\alpha^2 = \mu^2/2N = 0.2$ at $\nu = 0$. We show results for finite N versus numerical simulations. Both the eigenvalue densities for real eigenvalues $R^{\mathbb{R}}_{1,\mathrm{Dirac}}(x)$ and for pure imaginary ones $R^{\mathbb{R}}_{1,\mathrm{Dirac}}(\mathrm{i}x)$ are displayed in the same plot for comparison. Real density (upper curve): $N = 10$ (blue full line), $N = 20$ (dark green dot-dashed line); imaginary density (lower curve) $N = 10$ (red dashed line), $N = 20$ (black, dotted line). Dots with error bars: $N = 100$ Monte Carlo simulation of 10^4 matrices.

to strong eigenvalues is given by $\frac{z}{4\alpha^2} \to 2\eta_+ z$. Whilst the matching of the integrals over t is straightforward, the mapping of the kernels multiplied by the weight is more involved. Changing variables we have the following identity:

$$\begin{aligned}\alpha^2 \int_0^1 \mathrm{d}s\, s^2\, \mathrm{e}^{-2\alpha^2 s^2} \{\sqrt{z_1} J_{\nu+1}(s\sqrt{z_1}) J_\nu(s\sqrt{z_2}) - (z_1 \leftrightarrow z_2)\} \\ = 2\left(z_2 \frac{\partial}{\partial z_2} - z_1 \frac{\partial}{\partial z_1}\right) \int_0^\alpha \mathrm{d}t\; t\, \mathrm{e}^{-2t^2} J_\nu\left(t\frac{\sqrt{z_1}}{\alpha}\right) J_\nu\left(t\frac{\sqrt{z_2}}{\alpha}\right) \\ \to \frac{1}{2}\left(z_2 \frac{\partial}{\partial z_2} - z_1 \frac{\partial}{\partial z_1}\right) \exp\left[-\frac{(z_1+z_2)}{8\alpha^2}\right] I_\nu\left(\frac{\sqrt{z_1 z_2}}{4\alpha^2}\right) \end{aligned} \tag{4.29}$$

where in the last step we have extended the integral to infinity and used equation 6.633.2 of [34]. The last differentiation is trivial, in effect acting only on the exponential function. We thus obtain for the limiting kernel

$$\lim_{\alpha\to\infty} \alpha^4 \mathcal{K}^W(z_1, z_2)\big|_{\frac{z}{\alpha^2}\,\text{fixed}} = \left(\frac{z_1}{4\alpha^2} - \frac{z_2}{4\alpha^2}\right) \exp\left[-\frac{(z_1+z_2)}{8\alpha^2}\right] I_\nu\left(\frac{\sqrt{z_1 z_2}}{4\alpha^2}\right), \tag{4.30}$$

which precisely cancels the exponentials from the weight equation (4.21) to arrive at the complex density at strong non-Hermiticity equation (4.18).

We now turn to the real density at weak non-Hermiticity. Looking at the definitions equations (4.13) and (4.14) the main difference to the complex density is that here the kernel is integrated, whereas the complex density is simply given by the kernel multiplied by the weight.

Unfortunately, and in contrast to the strong non-Hermitian case, at weak non-Hermiticity, the large-N limit and the integration do *not* commute, with the integral over the weak kernel (4.27) not being absolutely convergent. Such a feature might have been expected, as the same phenomenon occurs for the chGOE at $\mu = 0$ [35]. However, in that case, the integrals could be computed exactly before taking the large-N limit, leading to the correct result, which differs from the naive limit by a factor of 2 in the normalization[9]. The integrals in equation (4.14) at finite N are more involved, and this matter will be addressed in future work.

[9] A quick guess generalizing this to our setting fails.

For that reason, we show in figure 6 the real density for finite but large $N = 10$ and 20, using the weak scaling from equation (4.26) and equation (4.20) for a given α. This underlines that the weak limit for the real density does exist and convergence is rapid. Furthermore, we have checked this by superimposing data for $N = 100$ using numerically generated random matrices.

As a feature common to the strong limit, we note that the densities of real and purely imaginary eigenvalues in figure 6 resemble cuts through the complex density in figure 5 left at the same value of $\alpha^2 = 0.2$.

5. Conclusions

In this paper we have solved the chiral extension of the Ginibre ensemble of real asymmetric matrices. It is given as a two-matrix model of rectangular matrices with real elements and depends on a non-Hermiticity parameter μ. This model is relevant for computing the non-Hermitian spectrum of Dirac operators with real elements in field theory. Our work completes the programme of solving the three chiral or Wishart–Laguerre counterparts of the classical Ginibre ensembles, where earlier works by Osborn and one of the authors extended the models with complex and quaternion real elements, respectively.

Whilst our model inherits most of the integrable structure of the real Ginibre ensemble, its joint probability distribution required a more complicated calculation, which took much of our effort here. Just as in the Ginibre ensembles, the probability density for the matrix elements is Gaussian, whereas the one for the eigenvalues becomes non-Gaussian. It contains a Bessel-K function and integral thereof, replacing the role of the complementary error function in the real Ginibre ensemble.

The main building block for all eigenvalue correlation functions is given by a kernel of Laguerre polynomials in the complex plane and was derived in a previous paper. Here, we give all eigenvalue density correlation functions for finite (even) N valid for all values of μ, in particular the spectral one-point densities for real eigenvalues and for complex non-real eigenvalues. Moreover, we have uncovered a way of expressing the $\beta = 1$ kernel in terms of the $\beta = 2$ kernel at finite and large N, both for the chiral and non-chiral Ginibre ensembles. We conjecture that a similar relation holds for the $\beta = 4$ kernel as well.

When taking microscopic large-N limits, we focus on the origin where the chiral symmetry of our model is the most important. For both the limit at strong non-Hermiticity with $0 < \mu^2 < 1$, and the limit at weak non-Hermiticity with $\mu^2 \sim 1/N$, we give compact expressions for the kernel. This leads to explicit expressions for the complex spectral one-point densities and the real density at strong non-Hermiticity.

It would be very interesting to compare these results with simulations from non-Hermitian lattice gauge theory, as was successfully done previously for the other two chiral two-matrix models.

Further extensions would be to investigate the bulk or the soft edge scaling limit. We expect that in the former, the chiral ensembles will agree with the Ginibre ensembles, as the effect of chirality becomes unimportant in the bulk.

Acknowledgments

This work has been supported partly by European Network ENRAGE MRTN-CT-2004-005616 (GA), an EPSRC doctoral training grant (MJP) and the SFB/TR12 of the Deutsche Forschungsgemeinschaft (H-JS). We thank Tilo Wettig for useful discussions.

Appendix A. Details on the calculation of the Jacobian

In this appendix, we give a few more details to complete the computation of the Jacobian from section 3.3. In particular, we first give a precise ordering of matrix elements leading to a block-triangular Jacobian. Second we will treat the case of non-diagonal matrices Λ_A and Λ_B.

For the first purpose, we repeat equation (3.37) including matrix indices, after dropping the outside rotations:

$$(\mathrm{d}A)_{ij} = \sum_{k=1}^{N} \left(O_A^T\,\mathrm{d}O_A\right)_{ik}(\Delta_A+\Lambda_A)_{kj} - \sum_{k=1}^{N+\nu}(\Delta_A+\Lambda_A)_{ik}\left(O_B^T\,\mathrm{d}O_B\right)_{kj} + (\mathrm{d}\Delta_A)_{ij} + (\mathrm{d}\Lambda_A)_{ij}, \tag{A.1}$$

$$(\mathrm{d}B^T)_{ij} = \sum_{k=1}^{N+\nu} \left(O_B^T\,\mathrm{d}O_B\right)_{ik}(\Delta_B+\Lambda_B)_{kj} - \sum_{k=1}^{N}(\Delta_B+\Lambda_B)_{ik}\left(O_A^T\,\mathrm{d}O_A\right)_{kj} + (\mathrm{d}\Delta_B)_{ij} + (\mathrm{d}\Lambda_B)_{ij}. \tag{A.2}$$

We now give an ordering leading to a block-triangular Jacobi matrix, with variables $\{\mathrm{d}A, \mathrm{d}B^T\}$ in the columns and $\left\{\mathrm{d}\Lambda_A, \mathrm{d}\Lambda_B, \mathrm{d}\Delta_A, \mathrm{d}\Delta_B, O_A^T\,\mathrm{d}O_A, O_B^T\,\mathrm{d}O_B\right\}$ in the rows. For the block diagonal matrices $\Lambda_{A,B}$ and upper block-diagonal matrices $\Delta_{A,B}$ (of different size), this is trivial: we just group them together with the corresponding elements of $\mathrm{d}A$ and $\mathrm{d}B^T$. For example, when N is even and $\nu > 0$, this will give

$$(\mathrm{d}A)_{11}, (\mathrm{d}A)_{12}, (\mathrm{d}A)_{21}, (\mathrm{d}A)_{22}, (\mathrm{d}A)_{33}, \ldots, (\mathrm{d}A)_{NN}, (\mathrm{d}B^T)_{11}, \ldots, (\mathrm{d}B^T)_{NN}, (\mathrm{d}A)_{13}, (\mathrm{d}A)_{14}, \ldots, (\mathrm{d}A)_{1,N+\nu}, (\mathrm{d}A)_{23}, \ldots, (\mathrm{d}A)_{N,N+\nu}, (\mathrm{d}B^T)_{13}, \ldots, (\mathrm{d}B^T)_{N-2,N} \tag{A.3}$$

versus

$$(\mathrm{d}\Lambda_A)_{11}, (\mathrm{d}\Lambda_A)_{12}, (\mathrm{d}\Lambda_A)_{21}, (\mathrm{d}\Lambda_A)_{22}, (\mathrm{d}\Lambda_A)_{33}, \ldots, (\mathrm{d}\Lambda_A)_{NN}, (\mathrm{d}\Lambda_B)_{11}, \ldots, (\mathrm{d}\Lambda_B)_{NN}, (\mathrm{d}\Delta_A)_{13}, (\mathrm{d}\Delta_A)_{14}, \ldots, (\mathrm{d}\Delta_A)_{1,N+\nu}, (\mathrm{d}\Delta_A)_{23}, \ldots, (\mathrm{d}\Delta_A)_{N,N+\nu}, (\mathrm{d}\Delta_B)_{13}, \ldots, (\mathrm{d}\Delta_B)_{N-2,N}. \tag{A.4}$$

The resulting sub-Jacobi matrix is clearly the identity matrix, and the order we have picked is arbitrary as long as we pair $(\mathrm{d}A)_{ij}$ with $(\mathrm{d}\Lambda_A)_{ij}$ or $(\mathrm{d}\Delta_A)_{ij}$, and respectively for B.

It remains to order the matrix elements $\mathrm{d}A$ and $\mathrm{d}B^T$ below the block diagonal. In order to obtain sub-blocks as in equation (3.39), we will always pair $(\mathrm{d}A)_{ij}$ with the square part of $(\mathrm{d}B^T)_{ij}$, with $i > j$ and $i, j \in 1, \ldots, N$ and finish with the rectangular part of $(\mathrm{d}B^T)_{ij}$, with $i = N+1, \ldots, N+\nu$. For that we write the following partial differentials denoted by '|' from equations (A.1) and (A.2):

$$(\mathrm{d}A|)_{i>j} \equiv \sum_{p=1}^{p<j<i} \left(O_A^T\,\mathrm{d}O_A\right)_{ip}(\Delta_A)_{pj} - \sum_{q>i>j}^{N+\nu}(\Delta_A)_{iq}\left(O_B^T\,\mathrm{d}O_B\right)_{qj}, \tag{A.5}$$

$$(\mathrm{d}B^T|)_{i>j} \equiv \sum_{p=1}^{p<j<i} \left(O_B^T\,\mathrm{d}O_B\right)_{ip}(\Delta_B)_{pj} - \sum_{q>i>j}^{N}(\Delta_B)_{iq}\left(O_A^T\,\mathrm{d}O_A\right)_{qj}. \tag{A.6}$$

Here we have already used that $\Lambda_{A,B}$ are upper triangular and that $i > j$ lets only the independent elements of the orthogonal differentials appear (we have chosen the below block diagonal ones).

For the variables $\Delta_{A,B}$ below the block diagonal, in order not to interfere with the block diagonals equation (3.39), we introduce the following ordering of elements:

$$\begin{aligned}&(i,j) \prec (i,p) \text{ if } p < j,\\ &(i,j) \prec (q,j) \text{ if } q > i.\end{aligned} \tag{A.7}$$

Here $\prec$ implies that the matrix element (i,j) on the left, that is $(\mathrm{d}A)_{ij}$ $\left(\left(O_A^T\,\mathrm{d}O_A\right)_{ij}\right)$, has to appear before the one on the right[10]. Looking back to equations (A.5) and (A.6), this implies that the elements $(\mathrm{d}A)_{ij}$ and $(\mathrm{d}B^T)_{ij}$ that depend on the most elements of $\left(O_A^T\,\mathrm{d}O_A\right)_{ij}$ and $\left(O_B^T\,\mathrm{d}O_B\right)_{ij}$ will appear first, leading to a lower triangular structure. However, the ordering equation (A.7) is not unique. We will proceed 2×2 blockwise (plus 1×2 blocks for the last row when N is odd) going down the diagonal, in order to preserve the block-diagonal structure when the matrices $\Lambda_{A,B}$ are not diagonal.

We thus continue the labelling in equations (A.3) and (A.4) as

$$\begin{aligned}&(\mathrm{d}A)_{32}, (\mathrm{d}B^T)_{32}, (\mathrm{d}A)_{31}, (\mathrm{d}B^T)_{31}, (\mathrm{d}A)_{42}, (\mathrm{d}B^T)_{42}, (\mathrm{d}A)_{41}, (\mathrm{d}B^T)_{41}, (\mathrm{d}A)_{54}, (\mathrm{d}B^T)_{54}, \ldots,\\ &(\mathrm{d}A)_{N1}, (\mathrm{d}B^T)_{N1}\end{aligned} \tag{A.8}$$

versus

$$\begin{aligned}&\left(O_A^T\,\mathrm{d}O_A\right)_{32}, \left(O_B^T\,\mathrm{d}O_B\right)_{32}, \left(O_A^T\,\mathrm{d}O_A\right)_{31}, \left(O_B^T\,\mathrm{d}O_B\right)_{31}, \left(O_A^T\,\mathrm{d}O_A\right)_{42}, \left(O_B^T\,\mathrm{d}O_B\right)_{42},\\ &\left(O_A^T\,\mathrm{d}O_A\right)_{41}, \left(O_B^T\,\mathrm{d}O_B\right)_{41}, \left(O_A^T\,\mathrm{d}O_A\right)_{54}, \left(O_B^T\,\mathrm{d}O_B\right)_{54}, \ldots, \left(O_A^T\,\mathrm{d}O_A\right)_{N1}, \left(O_B^T\,\mathrm{d}O_B\right)_{N1}.\end{aligned} \tag{A.9}$$

It remains for us to order the rectangular part of $(\mathrm{d}B^T)_{ij}$ with $i = N+1,\ldots,N+\nu$ versus the corresponding $\left(O_B^T\,\mathrm{d}O_B\right)_{ij}$. Using the same order as in equation (A.7), we complete our Jacobi matrix by

$$(\mathrm{d}B^T)_{N+1,N}, (\mathrm{d}B^T)_{N+1,N-1}, \ldots, (\mathrm{d}B^T)_{N+1,1}, (\mathrm{d}B^T)_{N+2,N}, \ldots, (\mathrm{d}B^T)_{N+\nu,1} \tag{A.10}$$

versus

$$\begin{aligned}&\left(O_B^T\,\mathrm{d}O_B\right)_{N+1,N}, \left(O_B^T\,\mathrm{d}O_B\right)_{N+1,N-1}, \ldots, \left(O_B^T\,\mathrm{d}O_B\right)_{N+1,1}, \left(O_B^T\,\mathrm{d}O_B\right)_{N+2,N}, \ldots,\\ &\left(O_B^T\,\mathrm{d}O_B\right)_{N+\nu,1}.\end{aligned} \tag{A.11}$$

In the second part of this appendix, we will deal with the case of $\Lambda_{A,B}$ being 2×2 block matrices rather than diagonal, which was omitted in section 3.3. We start with N even, and first only deal with the matrix elements $\mathrm{d}A$ and the square part of $\mathrm{d}B^T$ below the block diagonal (equations (A.8) and (A.9)). In this case it is no longer sufficient to study one pair of neighbouring elements as in equation (3.39), but rather four pairs. This leads to the following 8×8 matrix with the order chosen above. In the columns, we put $(\mathrm{d}A)_{i,j+1}$, $(\mathrm{d}B^T)_{i,j+1}$, $(\mathrm{d}A)_{ij}$, $(\mathrm{d}B^T)_{ij}$, $(\mathrm{d}A)_{i+1,j+1}$, $(\mathrm{d}B^T)_{i+1,j+1}$, $(\mathrm{d}A)_{i+1,j}$, $(\mathrm{d}B^T)_{i+1,j}$, and in the rows the elements $(O_A^T\,\mathrm{d}O_A)_{ij}$ and $(O_B^T\,\mathrm{d}O_B)_{ij}$ in the corresponding order. Using equations (A.1) and (A.2), this leads to the following sub-matrices down the diagonal for each odd i and odd j:

$$\begin{pmatrix}
(\Lambda_A)_{j+1,j+1} & -(\Lambda_B)_{ii} & (\Lambda_A)_{j+1,j} & 0 & 0 & -(\Lambda_B)_{i+1,i} & 0 & 0\\
-(\Lambda_A)_{ii} & (\Lambda_B)_{j+1,j+1} & 0 & (\Lambda_B)_{j+1,j} & -(\Lambda_A)_{i+1,i} & 0 & 0 & 0\\
(\Lambda_A)_{j,j+1} & 0 & (\Lambda_A)_{jj} & -(\Lambda_B)_{ii} & 0 & 0 & 0 & -(\Lambda_B)_{i+1,i}\\
0 & (\Lambda_B)_{j,j+1} & -(\Lambda_A)_{ii} & (\Lambda_B)_{jj} & 0 & 0 & -(\Lambda_A)_{i+1,i} & 0\\
0 & -(\Lambda_B)_{i,i+1} & 0 & 0 & (\Lambda_A)_{j+1,j+1} & -(\Lambda_B)_{i+1,i+1} & (\Lambda_A)_{j+1,j} & 0\\
-(\Lambda_A)_{i,i+1} & 0 & 0 & 0 & -(\Lambda_A)_{i+1,i+1} & (\Lambda_B)_{j+1,j+1} & 0 & (\Lambda_B)_{j+1,j}\\
0 & 0 & 0 & -(\Lambda_B)_{i,i+1} & (\Lambda_A)_{j,j+1} & 0 & (\Lambda_A)_{jj} & -(\Lambda_B)_{i+1,i+1}\\
0 & 0 & -(\Lambda_A)_{i,i+1} & 0 & 0 & (\Lambda_B)_{j,j+1} & -(\Lambda_A)_{i+1,i+1} & (\Lambda_B)_{jj}
\end{pmatrix}. \tag{A.12}$$

[10] Our ordering is different from appendix A.37 in [31] for the real Ginibre ensemble.

We can easily verify (using the symbolic manipulation capabilities of Mathematica [36], for example) that the modulus of the determinant of this is identical to

$$\mathcal{J}_{ij} = |(D_i - D_j)^2 + (S_i - S_j)(S_i D_j - S_j D_i)| \tag{A.13}$$

in which D_i is the determinant, and S_i the trace, of the 2×2 matrix U_i given by (only relevant for odd i)

$$U_i \equiv \begin{pmatrix} (\Lambda_A)_{ii} & (\Lambda_A)_{i,i+1} \\ (\Lambda_A)_{i+1,i} & (\Lambda_A)_{i+1,i+1} \end{pmatrix} \begin{pmatrix} (\Lambda_B)_{ii} & (\Lambda_B)_{i,i+1} \\ (\Lambda_B)_{i+1,i} & (\Lambda_B)_{i+1,i+1} \end{pmatrix}. \tag{A.14}$$

The same definition obviously applies for subscript j. However, D_i and S_i can of course be written in terms of the eigenvalues of U_i, which we denoted as Λ_i^2 and Λ_{i+1}^2, i.e.

$$D_i = \det U_i = \Lambda_i^2 \Lambda_{i+1}^2, \qquad S_i = \operatorname{Tr} U_i = \Lambda_i^2 + \Lambda_{i+1}^2. \tag{A.15}$$

Substituting these into equation (A.13), and factorizing, gives

$$\mathcal{J}_{ij} = \left|\left(\Lambda_i^2 - \Lambda_j^2\right)\left(\Lambda_{i+1}^2 - \Lambda_j^2\right)\left(\Lambda_i^2 - \Lambda_{j+1}^2\right)\left(\Lambda_{i+1}^2 - \Lambda_{j+1}^2\right)\right|. \tag{A.16}$$

This is exactly what we got in the case when the Λ_A and Λ_B matrices were diagonal, i.e. the product of four copies of equation (3.39), one for each of the combinations (i, j), $(i + 1, j)$, $(i, j + 1)$ and $(i + 1, j + 1)$.

When N is odd, we can treat the 2×2 blocks up to $N - 1$ (inclusive) as before. We still have to consider the final column of $\mathrm{d}A$, etc, and it is necessary here to treat (j, N) and $(j + 1, N)$ together as 2×1 blocks (for odd values of j in the range $1 \leqslant j < N$). Hence, we have extra diagonal blocks in the Jacobian (for each odd j) of the form

$$\begin{pmatrix} (\Lambda_A)_{j+1,j+1} & -(\Lambda_B)_{NN} & (\Lambda_A)_{j+1,j} & 0 \\ -(\Lambda_A)_{NN} & -(\Lambda_B)_{j+1,j+1} & 0 & (\Lambda_B)_{j+1,j} \\ (\Lambda_A)_{j,j+1} & 0 & (\Lambda_A)_{jj} & -(\Lambda_B)_{NN} \\ 0 & (\Lambda_B)_{j,j+1} & -(\Lambda_A)_{NN} & (\Lambda_B)_{jj} \end{pmatrix} \tag{A.17}$$

which is in fact the first sub-block of equation (A.12) with $i = N$. The modulus of the determinant of this is identically equal to

$$\mathcal{J}_{Nj} = \left|D_j - S_j \Lambda_N^2 + \Lambda_N^4\right|, \tag{A.18}$$

where we used that $(\Lambda_A)_{NN}(\Lambda_B)_{NN} = \Lambda_N^2$ (no sums), and D_j and S_j were defined as before. But we can switch to writing D_j and S_j in terms of the eigenvalues of U_j and this gives

$$\mathcal{J}_{Nj} = \left|\left(\Lambda_N^2 - \Lambda_j^2\right)\left(\Lambda_N^2 - \Lambda_{j+1}^2\right)\right|. \tag{A.19}$$

We see that this is again of the expected form.

Let us turn to the remaining variables, the rectangular part of $\mathrm{d}B^T$ in equations (A.10) and (A.11). We first suppose that N is even. For each i and each odd j we find that the variables $(\mathrm{d}B^T)_{i,j+1}$, $(\mathrm{d}B^T)_{ij}$ and $\left(O_B^T\,\mathrm{d}O_B\right)_{i,j+1}$, $\left(O_B^T\,\mathrm{d}O_B\right)_{ij}$ are now coupled into the following 2×2 blocks:

$$\begin{pmatrix} (\Lambda_B)_{j+1,j+1} & (\Lambda_B)_{j+1,j} \\ (\Lambda_B)_{j,j+1} & (\Lambda_B)_{jj} \end{pmatrix}, \tag{A.20}$$

whose determinant is (after a relabelling $2j - 1 \to j$) simply $\det B_j$ (using the definition of B_j after equation (3.41)). This is independent of i which takes ν different values,

$N+1 \leqslant i \leqslant N+\nu$. We therefore have a total contribution to the Jacobian of

$$\prod_{j=1}^{N/2} |\det B_j|^{\nu} \quad \text{for } N \text{ even}, \tag{A.21}$$

which is exactly as before (equation (3.41)).

Finally, when N is odd, we just pick up an extra factor of $(\Lambda_B)_{NN}$ from each of the ν cells in the last column $(\mathrm{d}B^T)_{iN}$, and so

$$\prod_{j=1}^{(N-1)/2} |\det B_j|^{\nu} |(\Lambda_B)_{NN}|^{\nu} \quad \text{for } N \text{ odd}. \tag{A.22}$$

This ends the calculation for non-diagonal matrices $\Lambda_{A,B}$.

References

[1] Ginibre J 1965 *J. Math. Phys.* **6** 440
[2] Fyodorov Y V and Sommers H-J 2003 *J. Phys. A: Math. Gen.* **36** 3303 (arXiv:nlin.CD/0207051)
[3] Lehmann N and Sommers H-J 1991 *Phys. Rev. Lett.* **67** 941
[4] Edelman A 1997 *J. Multivariate Anal.* **60** 203
[5] Kanzieper E and Akemann G 2005 *Phys. Rev. Lett.* **95** 230201 (arXiv:math-ph/0507058)
Akemann G and Kanzieper E 2007 *J. Stat. Phys.* **129** 1159 (arXiv:math-ph/0703019)
[6] Sinclair C D 2007 *Int. Math. Res. Not.* rnm015 (arXiv:math-ph/0605006)
[7] Sommers H-J 2007 *J. Phys. A: Math. Theor.* **40** F671 (arXiv:0706.1671)
[8] Forrester P J and Nagao T 2007 *Phys. Rev. Lett.* **99** 050603 (arXiv:0706.2020 [cond-mat.stat-mech])
Forrester P J and Nagao T 2008 *J. Phys. A: Math. Theor.* **41** 375003 (arXiv:0806.0055 [math-ph])
[9] Borodin A and Sinclair C D 2007 (arXiv:0706.2670v2 [math-ph])
Borodin A and Sinclair C D 2008 (arXiv:0805.2986 [math-ph])
[10] Sommers H-J and Wieczorek W 2008 *J. Phys. A: Math. Theor.* **41** 405003 (arXiv:0806.2756 [cond-mat.stat-mech])
[11] Forrester P J and Mays A 2008 (arXiv:0809.5116v2 [math-ph])
[12] Shuryak E V and Verbaarschot J J M 1993 *Nucl. Phys.* A **560** 306 (arXiv:hep-th/9212088)
Verbaarschot J 1994 *Phys. Rev. Lett.* **72** 2531 (arXiv:hep-th/9401059v1)
[13] Stephanov M A 1996 *Phys. Rev. Lett.* **76** 4472 (arXiv:hep-lat/9604003)
[14] Halasz M A, Osborn J C and Verbaarschot J J M 1997 *Phys. Rev.* D **56** 7059 (arXiv:hep-lat/9704007)
[15] Splittorff K and Verbaarschot J J M 2004 *Nucl. Phys.* B **683** 467 (arXiv:hep-th/0310271v3)
[16] Osborn J C 2004 *Phys. Rev. Lett.* **93** 222001 (arXiv:hep-th/0403131)
[17] Akemann G 2003 *J. Phys. A: Math. Gen.* **36** 3363 (arXiv:hep-th/0204246)
[18] Akemann G, Osborn J C, Splittorff K and Verbaarschot J J M 2005 *Nucl. Phys.* B **712** 287 (arXiv:hep-th/0411030)
[19] Akemann G 2005 *Nucl. Phys.* B **730** 253 (arXiv:hep-th/0507156)
Akemann G and Basile F 2007 *Nucl. Phys.* B **766** 150 (arXiv:math-ph/0606060)
[20] Akemann G, Phillips M J and Sommers H-J 2009 *J. Phys. A: Math. Theor.* **42** 012001 (arXiv:0810.1458v1 [math-ph])
[21] Verbaarschot J J M 2004 *Les Houches Summer School (France, 6–25 June)* (arXiv:hep-th/0502029v1)
Akemann G 2007 *Int. J. Mod. Phys.* A **22** 1077 (arXiv:hep-th/0701175)
[22] Bernard D and LeClair A 2001 A classification of non-Hermitian random matrices *proc. NATO Advanced Research Workshop on Statistical Field Theories (Como, 18–23 June)* (arXiv:cond-mat/0110649)
Magnea U 2008 *J. Phys. A: Math. Theor.* **41** 045203 (arXiv:0707.0418v2 [math-ph])
[23] Forrester P J and Mays A 2009 (arXiv:0910.2531 [math-ph])
[24] Edelman A, Kostlan E and Shub M 1994 *J. Am. Math. Soc.* **7** 247
[25] Akemann G and Vernizzi G 2003 *Nucl. Phys.* B **660** 532 (arXiv:hep-th/0212051)
[26] Tracy C A and Widom H 1998 *J. Stat. Phys.* **92** 809
[27] Forrester P J, Nagao T and Honner G 1999 *Nucl. Phys.* B **553** 601 (arXiv:cond-mat/9811142v1 [cond-mat.mes-hall])
[28] Efetov K B 1997 *Phys. Rev. Lett.* **79** 491 (arXiv:cond-mat/9702091 [cond-mat.dis-nn])
[29] Sommers H-J, Crisanti A, Sompolinsky H and Stein Y 1988 *Phys. Rev. Lett.* **60** 1895

[30] Fyodorov Y V, Khoruzhenko B A and Sommers H-J 1998 *Ann. Inst. Henri Poincaré* **68** 449 (arXiv:chao-dyn/9802025)
[31] Mehta M L 2004 *Random Matrices* 3rd edn (London: Academic)
[32] Fyodorov Y V, Khoruzhenko B A and Sommers H-J 1997 *Phys. Lett.* A **226** 46 (arXiv:cond-mat/9606173)
Fyodorov Y V, Khoruzhenko B A and Sommers H-J 1997 *Phys. Rev. Lett.* **79** 557 (arXiv:cond-mat/9703152)
[33] Abramowitz M and Stegun I E 1965 *Handbook of Mathematical Functions* (New York: Dover)
[34] Gradshteyn I S and Ryzhik I M 2000 *Table of Integrals, Series and Products* 6th edn (London: Academic)
[35] Verbaarschot J 1994 *Nucl. Phys.* B **426** 559 (arXiv:hep-th/9401092v1)
[36] Wolfram Research Inc. 2008 *Mathematica Version 7.0* (Champaign, IL: Wolfram Research)